ELSEVIER

Ore Geology Reviews 10 (1996) 135–177

ORE GEOLOGY REVIEWS

Formation of volcanogenic massive sulfide deposits: The Kuroko perspective

Hiroshi Ohmoto

Department of Geosciences, The Pennsylvania State University, University Park, PA 16802, USA
Institute of Mineralogy, Petrology and Economic Geology, Faculty of Science, Tohoku University, Sendai, 980-77, Japan

Received 7 February 1995; accepted 21 July 1995

Abstract

The main objective of this paper is to identify the geochemical, hydrological, igneous and tectonic processes that led to the variations in the physical (size, geometry) and chemical (mineralogy, metal ratios and zoning) characteristics of volcanogenic massive sulfide deposits with respect to space (from a scale of mining district size area to a global scale) and time (from a $< 10\,000$ year time scale to a geologic time scale).

All volcanogenic massive sulfide deposits (VMSDs) appear to have formed in extensional tectonic settings, such as at mid ocean spreading centers, backarc spreading centers, and intracontinental rifts (and failed rifts). All VMSDs appear to have formed in submarine depressions by seawater that became ore-forming fluids through interactions with the heated upper crustal rocks. Submarine depressions, especially those created by submarine caldera formation and/or by large-scale tectonic activities (e.g., rifting), become most favorable sites for the formation of large VMSDs because of hydrological, physical and chemical reasons.

The fundamental processes leading to the formation of VMSDs include the following six processes:

(1) Intrusion of a heat source (typically a $\sim 10^3$ km size pluton) into an oceanic crust or a submarine continental crust causes deep convective circulation of seawater around the pluton. The radius of a circulation cell is typically ~ 5 km. The temperature of fluids that discharge on the seafloor increases with time from the ambient temperature to a typical maximum of ~ 350°C, and then decreases gradually to the ambient temperatures in a time scale of ~ 100 to $\sim 10\,000$ years. The majority of sulfide and sulfate mineralization occurs during the waxing stage of hydrothermal activity.

(2) Reactions between low temperature ($T < 150$°C) country rocks with downward percolating seawater cause to precipitate seawater SO_4^{2-} as disseminated gypsum and anhydrite in the country rocks.

(3) Reactions of the "modified" seawater with higher-temperature rocks at depths during the waxing stage cause the transformation of the "seawater" to metal- and H_2S-rich ore-forming fluids. The metals and sulfide sulfur are leached from the county rocks; the previously formed gypsum and anhydrite are reduced by Fe^{2+}-bearing minerals and organic matter, providing additional H_2S. The mass of high temperature rocks that provide the metals and reduced sulfur is typically $\sim 10^{11}$ tons (~ 40 km^3 in volume). The roles of magmatic fluids or gases are minor in most massive sulfide systems, except for SO_2 to produce acid-type alteration in some systems.

(4) Reactions between the ore-forming fluids and cooler rocks in the discharge zone cause alteration of rocks and precipitation of some ore minerals in the stockwork ores.

(5) Mixing of the ore-forming fluids with local seawater within unconsolidated sediments and/or on the seafloor causes precipitation of "primitive ores" with the black ore mineralogy (sphalerite + galena + pyrite + barite + anhydrite).

(6) Reactions between the "primitive ores" with later and hotter hydrothermal fluids cause transformation of "primitive ores" to "matured ores" that are enriched in chalcopyrite and pyrite.

SSDI 0169-1368(95)00021-6

Variations in the mineralogical and elemental characteristics, the geometry, and the size of submarine hydrothermal deposits are controlled by the following four parameters:

(A) The chemical and physical characteristics of seawater (composition, temperature, density), which depend largely on the geographical settings (e.g., equatorial evaporating basins),

(B) The chemical and physical characteristics of the plumbing system (lithology, fractures),

(C) The thermal structure of the plumbing system, which is determined largely by the ambient geothermal gradient, and the size and temperature of the intrusive, and

(D) The physical characteristics of the seafloor (depth, basin topography).

For example, the submarine hydrothermal deposits developed in basaltic plumbing systems are generally poor in Pb and Ba compared to those developed in felsic plumbing systems. The lower temperature systems are generally poorer in sulfides, but richer in iron oxides and sulfates. The higher temperature and larger hydrothermal systems tend to produce chalcopyrite and pyrite rich ores. Contrasts in the metal ratios between the Noranda-type Archean VMSDs and the younger VMSDs reflect the differences in the geothermal gradient of the plumbing systems. The submarine hydrothermal deposits developed in the near equatorial regions tend to form large continuous bedded type ores because of the likeliness of creating large stratified basins.

The basic processes of submarine hydrothermal mineralization have remained essentially the same throughout the geologic history, from at least 3.5 billion year ago to the present.

1. Introduction

Many excellent review papers have been written on volcanogenic massive sulfide deposits (e.g., Hutchinson, 1973; Sangster and Scott, 1976; Franklin et al., 1981; Guilbert and Park, 1986) and on modern submarine hydrothermal mineralization at spreading centers (e.g., Rona, 1988; Rona and Scott, 1993). These review papers generally present descriptions of the geological and mineralogic characteristics of several important deposits and mining districts, and attempt to review *objectively* the geochemical data and various theories on ore genesis presented by previous investigators. My approach taken in this paper is, however, highly *subjective*, much like the approach taken by Solomon (Solomon, 1976; Solomon and Walshe, 1979; Solomon et al., 1987). I will attempt to identify what are the common characteristics (i.e., main themes) in many VMSDs and what are the variations of the main themes, and to present conceptional models that relate the observed characteristics to ore-forming processes. A special focus will be placed on a question "What determines the variations in the physical and chemical characteristics (e.g., size, geometry, metal ratios, zonings, alteration) of submarine hydrothermal deposits?"

Many of the concepts that will be presented in this paper are those developed by scientists involved in the US–Japan–Canada Cooperative Research Project on the Genesis of Volcanogenic Massive Sulfide Deposits. Details of the models and supporting data can be found mostly in papers within Economic Geology Monograph No. 5 (Ohmoto and Skinner, 1983), but some unpublished data and more recently developed concepts will also be introduced here.

The US–Japan–Canada Cooperative Research Project on VMSDs focused primarily on the Kuroko deposits in the Hokuroku district, Japan. "Kuroko" literally means "black ore" in Japanese and refers, sensu stricto, to a massive sulfide ore consisting mostly of sphalerite and galena. "Kuroko" is, however, frequently used in a looser and broader sense for volcanogenic massive sulfide deposits of Miocene age in Japan. These Kuroko deposits have played a key role in research on VMSDs. They are the longest studied group of VMSDs, the first recognized as being of submarine, exhalative origin (Ohashi, 1919), and those which have become the classical model, or type-defining example, for all VMSDs. The last Kuroko mine in Japan was closed down unfortunately in 1994 because the rising value of the yen had made it more economical to import foreign ores.

2. General characteristics of VMSDs

There are three important groups of basemetal deposits formed by hydrothermal processes under submarine conditions: volcanogenic massive sulfide deposits (VMSDs), shale/carbonate hosted massive

sulfide deposits (SHMSDs), and banded iron formations (BIFs). The distinction among these three groups of deposits has been made mostly on the basis of dominant lithology of the host and footwall rocks, geometry, especially the lateral extent, of ore bodies, and metal ratios of ores. However, distinction between VMSDs and SHMSDs is often difficult to make, especially for metamorphosed deposits. Many BIFs also exhibit many characteristics of VMSDs and SHMSDs.

Massive sulfide deposits that are associated with submarine volcanic rocks have been called by a variety of names, such as "volcanogenic massive sulfide deposits", "volcanic-associated massive sulfide deposits", "submarine exhalative deposits", and "Kuroko-type deposits". Commonly referred to as VMSDs, they occur in rocks of all ages, from the Archean to the present, and are important sources of Cu, Zn, Pb, Ag and Au in many countries. The deposits that are tabulated by the US Geological Survey (Mosier et al., 1983) as VMSDs total 509, excluding those in eastern Europe, the former Soviet Union and China. They are estimated to contain a total of about 4 billion tons of ore with an average grade of Cu = 1.5 wt%, Zn = 3 wt%, Pb = 1 wt%, Ag = 50 g/ton, and Au = 0.5 g/ton. In terms of economic importance, they rank second only to porphyry copper deposits among nonferrous metallic mineral deposits (Rose et al., 1977).

2.1. Geometry and size

An idealized cross-section of a VMSD is shown in Fig. 1. A typical VMSD consists of two major types of ore bodies: a stratiform and stratabound massive sulfide ore body where the sulfide contents generally exceed 50% by volume; and a stockwork (stringer, or siliceous) ore zone consisting of veinlets and disseminated mineralization in the footwall rock of the massive sulfide ore body (Fig. 1). Typically, more than 90% of the heavy metals in a deposit are found in the massive ore body, less than 10% in the stockwork zone. A massive sulfide ore body generally is mound shaped with typical dimensions of ~ 20 m in height and ~ 300 m in radius (i.e., a very small height/length ratio). The stockwork ore zone commonly is a downward-narrowing, funnel-shaped body with an average radius of ~ 100 m at the top and a downward length of ~ 100 m.

It is now generally accepted that the stockwork zone represents the channelways for the hydrothermal fluids, and that the massive ore represents an accumulation either on the seafloor and/or in unconsolidated sediments of sulfides, both of which were

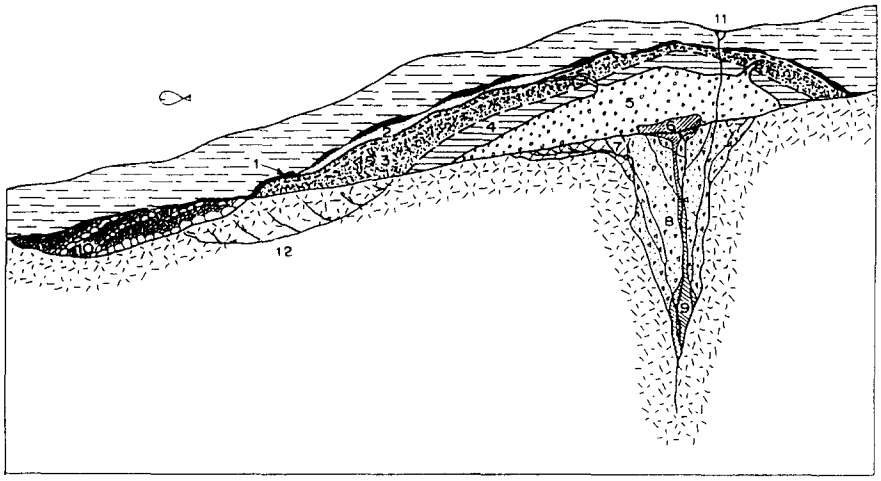

Fig. 1. An idealized representation of a relatively undisturbed Kuroko deposit. *1* = tetsusekiei or chert–hematite layer, *2* = barite ore, *3* = massive black ore, *4* = massive semiblack ore, *5* = massive yellow ore, *6* = massive pyrite ore, *7* = siliceous black ore, *8* = siliceous yellow ore, *9* = siliceous pyrite ore, *10* = transported, fragmented massive ore, *11* = late stage sulfide veins, *12* = gypsum/anhydrite ore. Modified after Eldridge et al., 1983.

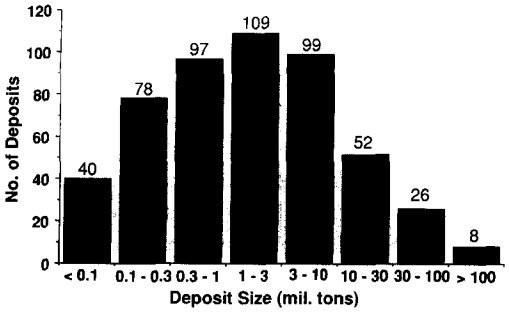

Fig. 2. Size distribution of the 509 volcanogenic massive sulfide deposits tabulated in Mosier et al. (1983).

formed by interactions between the discharged hydrothermal fluids and local cold seawater. That is, the stockwork ores are epigenetic, while the massive ores are mostly syngenetic.

An average Kuroko deposit is essentially identical to an average deposit of the 509 VMSDS in the world, containing about 1 million tons of ores with grades of 1.5 wt% Cu, 3 wt% Zn, 1 wt% Pb, 15 wt% Fe, 50 ppm Au and 0.5 ppm Au (Tanimura et al., 1983). When the tonnages of VMSDs are compared on a logarithmic scale, they show a near-normal frequency distribution with the mode lying between 1 and 3 million tons for 109 of 509 deposits (Fig. 2). Eight are "super giant" deposits with tonnages of ~ 100 to ~ 200 million tons: the Kidd Creek and the Horne deposits in the Abitibi belt, Canada (Archean age); the Mt. Lyell deposit in Tasmania, Australia (Cambrian); the Brunswick No. 12 deposit in New Brunswick, Canada (Ordovician); and four Carboniferous deposits (Rio Tinto, San Guillermo, Filon and La Zarza) in the Iberian pyrite belt. Super giant deposits discovered or reported their reserves since the compilation by Mosier et al. (1983) include the Proterozoic Crandon deposit in Wisconsin, USA (Lambe and Rowe, 1987), and the Carboniferous Aljustrel and the Neves–Corvo deposits in the Iberian pyrite belt (e.g., Munha et al., 1986). The modern metalliferous sediments in the Atlantis II Deep in the Red Sea (Amann et al., 1973; Pottorf and Barnes, 1983) represents another super giant VMSD. The ore body dimensions in these super giant deposits are obviously much greater than those in the average deposit. For example, the massive ore body at Kidd Creek is about 50 m in thickness and at least 1000 m diameter. The Rio Tinto ore body is about 150 m thick in the central zone and more than 800 m in diameter.

The dimension of a SHMSD is generally comparable to a VMSD. However, the number of economic-sized SHMSDs are only about 1/10 of VMSDs (Gustafson and Williams, 1981).

A large VMSD, such as the Rio Tinto and the Roseberry deposits, typically occurs solitary; the distance between large VMSDs is typically more than 10 km (Solomon and Walshe, 1979). However, a smaller VMSD seldom occurs solitary, but rather within a cluster of several ore bodies within an area of ~ 5 km^2 which constitutes a mining area. Several ore clusters are common in an area of ~ 1000 km^2, constituting a mining district. The total amount of ore in a mining district is typically about a few hundred million tons.

2.2. Associated rock types

The lithology of the host- and hangingwall rocks of the massive sulfide ore bodies varies among deposits, from clastic sediments (shale, sandstone) to volcanics (tuff, tuff breccia, lava); the *immediate footwall* rocks, however, are usually volcanics or intrusives (Fig. 1). Where the proportion of volcanic rocks is much less than that of clastic sediments in the rock sequence, the distinction between a VMSD and a shale/carbonate-hosted massive sulfide deposit becomes obscure. The examples include the Rammelsberg deposit in Germany and the Broken Hill deposit in Australia. Generally, deposits are classified as VMSDs if the thickness of more than ~ 10 m of volcanic rocks are found in the host- and/or in the immediate footwall rocks.

Sedimentary carbonates (limestones and dolomites) are not common in the host rock sequence of VMSDs, probably because the host rocks of VMSDs accumulated in deep oceans. From the foraminiferal assemblages found in the mudstones associated with the Kuroko deposits, Guber and Merrill (1983) have suggested that they accumulated near the carbonate compensation depth of around 3500–4000 m. A deep-sea environment, > 2000 m, has been suggested for the Cyprus deposits of Cretaceous age (Spooner and Fyfe, 1973). The depths at which base-metal sulfides are formed in the Red Sea

and along the mid oceanic ridges (e.g., the black smokers on the East Pacific Rise at 21°N, 13°N and 11°N) are also around 2500 m or deeper. In contrast, the host sediments of most shale/carbonate-hosted massive sulfide deposits, as indicated by ripple marks and other sedimentological features, appear to have accumulated in seas or lakes shallower than ~ 500 m in depth (Gustafson and Williams, 1981; Geer, 1988).

The footwall igneous rocks associated with VMSDs range from ultramafic to felsic in composition. The deposits occurring in dominantly mafic rocks of ophiolite sequences are often referred to as the Cyprus-type VMSDs, or more recently as Mid-ocean ridge type, while those associated with felsic igneous rocks or mixed-volcanics are referred to as the Kuroko type. The Besshi type or the Kieslager type are those occurring in a stratigraphic sequence dominated by clastic sediments with some mafic igneous rocks.

The VMSDs associated with dominantly felsic volcanic rocks are economically the most important group, accounting for 44% of Cu, 60% of Zn, 83% of Pb, and about 57% of Ag and Au production in the 509 VMSDs (Table 1). Those associated with mixed volcanics, where felsic volcanics are sub-equal to the intermediate and/or basaltic volcanics (i.e., bimodal volcanism), are the second most important group of VMSDs. Those associated with mostly mafic volcanics, i.e., the Cyprus- and the Besshi-type deposits, are economically the least important group; an exception is the Red Sea metalliferous deposits. The immediate footwall rocks of all other super-giant deposits are dominantly felsic volcanics.

The metal ratios of VMSDs vary depending on the associated volcanic rock types as indicated in Table 1: those associated with mafic volcanics tend to be higher in the Cu/Zn, Cu/Pb and Zn/Pb ratios than those associated with felsic volcanics.

2.3. Temporal and spatial distribution

The age distribution of VMSDs found worldwide is not uniform (Fig. 3). Deposits of the Silurian, Devonian, Permian and Triassic ages are few and economically less important than those of other ages; in contrast, the Ordovician- and Carboniferous-age VMSDs are economically more important than the others. Whether such an uneven age distribution of VMSDs reflects differences in formation, preservation and/or discovery, is difficult to evaluate, because the data in Fig. 3 are strongly influenced by the statistics in a handful of mining districts. For example, essentially all of the known Ordovician deposits are in the Bathurst district in Canada, the Carboniferous deposits in the Iberian pyrite belt, the

Table 1
Statistics for volcanogenic massive sulfide deposits

	Cu	Zn	Pb	Ag	Au
Average ore grade	1.4%	2.9%	0.7%	30 ppm	0.5 ppm
Total metals (mill. tons)	50	120	30	0.1	0.002
Percentage of the metals in:					
Phanerozoic deposits	60	62	91	62	72
Proterozoic deposits	17	14	5	11	21
Archean deposits	23	24	4	27	7
(Total)	(100)	(100)	(100)	(100)	(100)
Percentage of the metals in deposits associated with:					
Felsic volcanics	44	60	83	56	58
Mixed volcanics (bimodal)	32	26	9	30	13
Andesitic volcanics	13	12	7	12	20
Basaltic volcanics	11	2	1	2	9
(Total)	(100)	(100)	(100)	(100)	(100)

Data source: Mosier et al., 1983. Total number of deposits = 509. Total ore = 4 billion tons.)

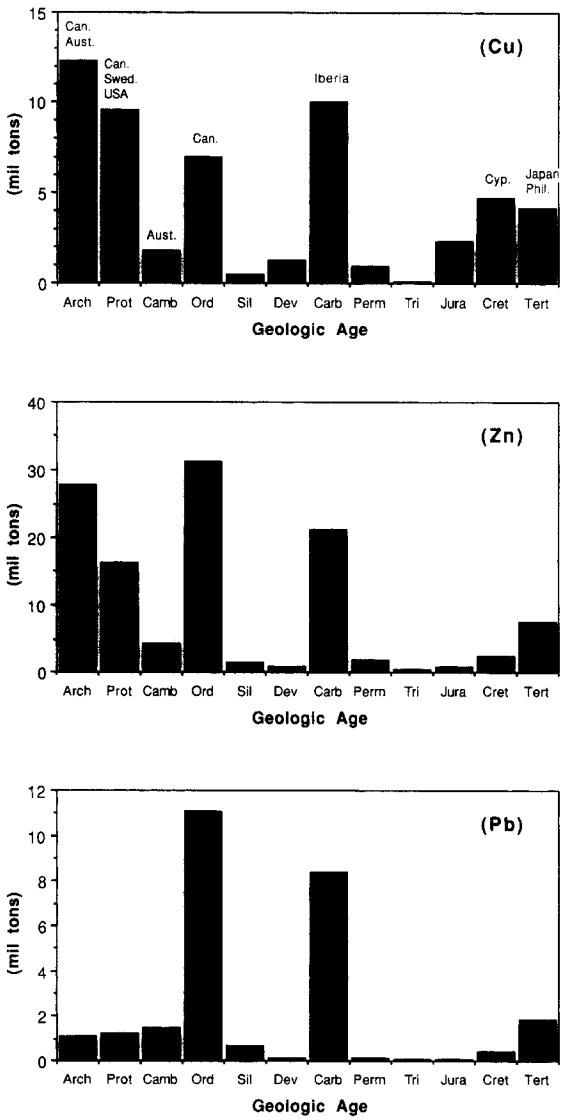

Fig. 3. Age distribution of the amounts of metals in the 509 volcanogenic massive sulfide deposits tabulated in Mosier et al. (1983). Also shown are major ore producing countries for VMSDs of different geologic ages. *Aust.* = Australia, *Can.* = Canada, *Cyp.* = Cyprus, *Phil.* = Phillippins, *Swed.* = Sweden.

Cretaceous deposits in Cyprus, and the Tertiary deposits in the Hokuroku district, Japan. If the erosional levels were deeper or shallower than the present levels by only ~500 m in some of these districts, the metal statistics of VMSDs would have been quite different from those shown in Fig. 3.

The age distribution of SHMSDs is much more restricted than that of VMSDs, and ranges from Proterozoic to Triassic (Gustafson and Williams, 1981). The reasons are not well understood as to why SHMSDs older than about 2.0 b.y. ago and those younger than about 150 m.y. ago have not been discovered.

Data summarized in Table 1 and Fig. 3 reveal a striking contrast in the metal ratios among VMSDs of different ages. Archean deposits tends to be poorer in Pb, as indicated by the fact that the Archean VMSDs account for only about 4% of the Pb, but 23–24% of the Cu and Zn in all VMSDs.

2.4. Zoning

Massive sulfide bodies in the Kuroko deposits are commonly zoned mineralogically and chemically (Fig. 1). A typical zoning sequence, from top to bottom, is: barite ore (barite > sulfides, in abundance), black ore or Zn–Pb-rich ore (sphalerite ≈ barite > pyrite ≈ galena), yellow ore or Cu-rich ore (chalcopyrite ≈ pyrite > sphalerite), and pyrite ore (nearly monomineralic). The stockwork zone is characterized by abundant quartz and rare barite; the sulfide zoning similar to that in the massive ores, but expressed laterally instead of vertically (i.e., pyrite-rich core, to yellow ore, and to peripheral black ore), may be present. Many of the massive sulfide ore bodies are overlain by thin (< ~ 1 m) and discontinuous layers of ferruginous chert, which is called "chert–hematite ore", "hematite–quartz ore", "tetsusekiei ore", or "exhalite". Massive bodies of gypsum/anhydrite are commonly developed underneath the massive sulfide ore body in the peripheral parts.

Mineralogical and chemical zoning similar to that in the Kuroko deposits is found in many other volcanogenic massive sulfide deposits, but with some noticeable variations. Those associated with mafic volcanics, regardless of age, and the Archean VMSDs in the Abitibi Greenstone Belt, Canada, regardless of the associated rock type, tend to contain appreciable amounts of pyrrhotite and magnetite, but lesser amounts of barite and galena. Gypsum/anhydrite bodies are also rare in the Canadian Archean deposits. However, barite- and galena-rich Archean

VMSDs have been discovered in the Pilbara district of western Australia.

2.5. Alteration of country rocks

Typical alteration zoning in the footwall rocks of a massive Kuroko ore body, from the central to the outer zone, consists of sericite/chlorite-, montmorillonite-, zeolite-II- and zeolite-I zones. The sericite/chlorite zone coincides fairly closely with the stockwork ore zone; the montmorillonite zone extends about 500 m outward from the stockwork zone; the zeolite-I zone represents the background alteration of submarine volcanics. The hydrothermal alteration (i.e., sericite/chlorite- and montmorillonite zones) commonly extends into the hanging-wall rocks of VMSDs, indicating that hydrothermal activity continued after the formation of sulfide ores.

3. Processes of ore growth

3.1. Previous models

Earlier studies on fluid inclusions in Kuroko samples (see Pisutha-Arnond and Ohmoto, 1983 for a review of data), although reconnaissance in nature, recognized two important characteristics of the ore-forming fluids: the temperatures were around 250°C, and the salinities were similar to those of normal seawater (i.e., ~ 3.5 wt% NaCl equivalent). As pointed out by Sato (1972) and Solomon and Walshe (1979), such fluids may rise like a plume when discharged into the overlying sea; their densities at $T \approx 250$°C are only about 0.7. Mixing of the plume fluids with cold seawater may cause ore minerals to crystallize out in the plume and settle on the seafloor (Solomon and Walshe, 1979). The discovery in 1978 of the black smokers at 21°N on the East Pacific Rise (Francheteau et al., 1979) appeared at first glance to support such a model.

The discovery of high-temperature brine pools and associated heavy-metal mineralization in the Red Sea (Miller et al., 1966; Degens and Ross, 1969) led to the development of another ore-growth model (e.g., Sato, 1972). Ore-forming fluids for some VMSDs were more saline, and, therefore, denser than normal seawater even at high temperatures. Such fluids may form a high-temperature brine pool when emerging at the seafloor. Slow cooling of the brine pool, due to the conductive loss of heat to the overlying cooler seawater, may cause ore minerals to crystallize out at the top of the brine pool and settle on the seafloor. Sulfide ore bodies formed in such brine pools may, therefore, have much larger lateral dimensions than the Kuroko-type deposits. For example, in the Atlantis II Deep of the Red Sea, there are two unconsolidated sulfide mud layers of 2 to 4 m thick over an area of 5×14 km (Degens and Ross, 1969; Pottorf and Barnes, 1983) (see later section on "Hydrology of the Plumbing System").

In both the plume and brine-pool models, it was believed that the massive sulfide ores accumulated on the seafloor simply from the bottom to top, much like snow accumulates on the ground. The massive pyrite ore, therefore, was believed to be older than the Cu-rich yellow ore, and the yellow ore older than the Zn-rich black ore. Various theories have been presented to explain why the dominant sulfide mineralogy changed during the accumulation of a VMSD (see Eldridge et al., 1983, for a review). Among the more popular was a theory suggesting a change with time in the chemical composition of discharging hydrothermal fluids: the earliest discharging fluids were richer in Fe, followed by Cu-rich fluids, and then by Cu-poor and Zn-rich fluids (e.g., Sato, 1973; Solomon and Walshe, 1979). Such changes in fluid chemistry may have been caused by the change in the temperatures of fluids, from the earlier higher temperatures to later cooler temperatures.

One of the serious problems with the previous models, however, has been the difficulty in explaining why the earlier fluids did not form Zn- and Pb sulfides, but only pyrite and/or chalcopyrite. Because the solubilities of sphalerite and galena in chloride complexes increase rapidly with increasing temperatures, the earlier (hotter?) fluids must have transported much more Zn and Pb than the later fluids. A possible reason for the low amount of shalerite and galena has been suggested by Solomon and Walshe (1979) and Solomon (pers. commun., 1995) as follows: The hotter fluids would have had somewhat higher buoyancy relative to seawater and the peak of temperature would have coincided more or less with maximum mass flux (the most important factor influencing velocity). Hence velocities in the

plumes would have been substantially higher, with increased chances of removal of galena and sphalerite precipitated at higher levels in the plume fluids than the Cu–Fe minerals.

3.2. New model

Systematic investigations of the mineralogy and fluid inclusions of the Kuroko deposits, carried out by Eldridge et al. (1983) and Pisutha-Arnond and Ohmoto (1983), have recognized several important features contradicting the previous ore-growth models. For example, most of the black ore minerals (sphalerite, galena, tetrahedrite, barite, pyrite) appear to have formed during the *earlier*, *waxing* stage of hydrothermal activity at temperatures of ~ 200° to ~ 300°C, but most of the Cu-bearing minerals (chalcopyrite, bornite) formed as *replacement* products of the black-ore minerals during the thermal-maximum stage at temperatures of ~ 280° to ~ 380°C. Only minor amounts of the black-ore minerals were formed during the waning stage of hydrothermal activity, at temperatures of ~ 300° to ~ 150°C (Fig. 4). The most important difference between the previous and the new models is whether most of the Cu-sulfide minerals were primary precipitates from hydrothermal solutions or replacements of the black-ore sulfides.

The initial phase of chalcopyrite replacement of sphalerite, which appears as minute inclusions of chalcopyrite along fractures and in iron-rich zones of sphalerite, was first recognized by Barton (1978) in samples from the Kuroko deposits through the use of doubly polished thin sections, and was termed "chalcopyrite disease". Chalcopyrite disease, which suggests Cu mineralization was later than Zn mineralization, turns out to be a very common phenomenon in VMSDs, as well as in other types of sulfide deposits (Eldridge et al., 1983; Barton and Bethke, 1987).

The new ore-growth model that takes into account the paragenesis and thermal history of the Kuroko

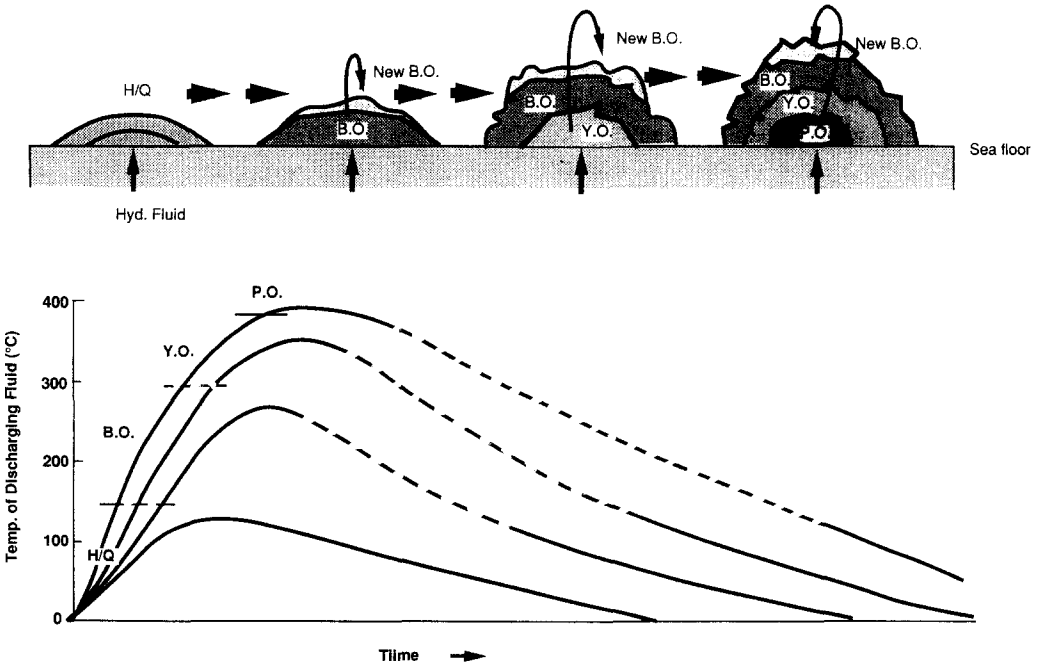

Fig. 4. Model for maturation of a volcanogenic massive sulfide deposit (top), and thermal history of discharging hydrothermal fluid (bottom). *H / Q* = hematite + quartz ore, *B.O.* = black ore (sphalerite + galena + pyrite + anhydrite + barite), *Y.O.* = yellow ore (chalcopyrite), *P.O.* = massive pyrite ore.

deposits and the sulfide chimneys from the East Pacific Rise (e.g., Goldfarb et al., 1983; Graham et al., 1988) is illustrated in Fig. 4. It postulates that massive sulfide ores grew by two principal processes. The first process is the rapid mixing of hydrothermal fluids with cold seawater at the top of ore mounds or at the exterior of chimney walls. This process results in the formation of the "primitive black ore" or "facies-1 ore", which is comprised of fine-grained (< 50 microns) mixtures of anhydrite–barite–sphalerite–galena–pyrite–tetrahedrite in the Kuroko deposits, or anhydrite–wurtzite–marcasite in the EPR chimneys (Graham et al., 1988). The second process is the reaction of the "primitive" black-ore minerals with the late and increasingly hotter hydrothermal fluids. This process progressively alters the pre-existing minerals, downward in ore mounds or inward in the chimney walls, by: dissolution of the primitive black ore minerals, recrystallization of the primitive black ore to coaser-grained black ore (facies-2 ore), and replacement of facies-2 minerals by chalcopyrite (facies-3 ore). The black-ore metals which were dissolved from the interior of ore mounds (or chimney walls) by later fluids are partially redeposited when the fluids mixed with cold seawater at or near the exterior surface of an ore body. When most of the black ore minerals are dissolved away from the lower parts of the ore pile, chalcopyrite begins to be dissolved by later fluids and replaced by new pyrite. Thus, Ca, Ba, Zn, Fe, Pb and S are continuously added to the exterior of a massive ore body during heating, while new Cu and Fe is added to the interior. The ore-growth processes for VMSDs, in a way, may be considered analogous to the skarn-forming processes, in which reaction fronts continuously migrate outward, and the earlier minerals are continuously transformed metasomatically by the later fluids. The only difference from the skarn-forming processes is the external media, with which hydrothermal solutions interact, local seawater instead of limestone.

During the earliest and low-temperature ($T <$ 150°C) stage of hydrothermal activity, some hematite ores may have formed on the seafloor; but they were probably replaced by sulfides during the waxing stage (Fig. 4). The most common type of hematite ores is that formed during the waning stage of hydrothermal activity.

3.3. Precipitation of minerals during mixing of hydrothermal fluids with local seawater

An accurate evaluation of the amounts of minerals that may precipitate during the interaction of hydrothermal fluids and cold seawater is difficult, unless the chemistry of the hydrothermal fluids is known for each stage of hydrothermal activity, and thermodynamic and kinetic information is available for all of the pertinent reactions. Lacking this information, it is possible, however, to evaluate qualitatively which minerals are likely or not likely to precipitate during the interaction of hydrothermal fluids and cold seawater. Comparison of the results obtained from such calculations with the observed mineral abundances in the ores may, in turn, put important constraints on the composition of hydrothermal fluids and on the mechanisms of ore growth.

When hot hydrothermal fluid and cold seawater encounter each other, transfer of heat and matter take place between the two fluids until they become identical in temperature and compositions. Types of mineralization accompanying fluid interaction may depend on the relative rates of heat and mass transfer between the two fluids, and nucleation of minerals. An end-member case is conductive cooling without mixing where the rate of mass transfer, at least initially, is much slower than that of heat transfer, each fluid acts simply as a coolant or heater for the other fluid, resulting in some mineral (e.g., sulfides) precipitating from the cooled hydrothermal fluids, while other minerals (e.g., anhydrite) precipitate from the heated seawater. Another end-member case is a very rapid mixing of two fluids (e.g., stirring of cold seawater into hot hydrothermal fluids), where the transfer rates of heat and fluid components (e.g., Na, ΣSO_4^{2-}, H^+, H_2) are essentially identical; the cooling rate is proportional to the fraction of cold water in the fluid mixtures, and minerals precipitate from the fluid mixtures. The first question is, therefore, which type of fluid interaction was responsible for the precipitation of the "primitive" black-ore minerals.

3.3.1. Sulfate minerals

The stoichiometric solubility of anhydrite decreases rapidly with increasing temperature, while

that of barite increases with increasing temperature (e.g., Holland and Malinin, 1979). Therefore, simple heating of seawater by hot fluid without fluid mixing may precipitate anhydrite, while simple cooling of hydrothermal solutions by cold seawater may precipitate barite. If this was the case in VMSDs, the sulfur and oxygen isotopic compositions of anhydrite should be essentially identical to those of SO_4^{2-} in local seawater, while those in barite similar to SO_4^{2-} in hydrothermal fluids.

However, most anhydrite and barite in the primitive black ore of the Kuroko deposits exhibit sulfur and oxygen isotopic compositions that are intermediate between those of the normal Miocene seawater sulfate ($\delta^{34}S = +20‰$ and $\delta^{18}O = +10‰$) and those of sulfate in hydrothermal fluids ($\delta^{34}S = \sim +28‰$ and $\delta^{18}O = \sim +6‰$; Ohmoto et al., 1983) (see also Fig. 15). This suggests that the primitive black-ore minerals crystallized from *mixtures* of hydrothermal fluids and local seawater, and that the ΣSO_4^{2-} content of the Kuroko ore-forming fluids was similar to that of normal seawater ($\sim 10^{-2}$ *m*).

Since the Ba content of the Kuroko ore-forming fluids was most likely greater than 10^{-5} *m* (Table 2), while that in normal seawater is only $\sim 10^{-8}$ *m*, barite formation in the primitive black ore may be written as:

$$Ba^{2+}(\text{hyd.fl.}) + X SO_4^{2-}(\text{hyd.fl}) + (1-X)SO_4^{2-}(\text{local s.w.}) \Rightarrow BaSO_4(s) \quad (1)$$

where X is the mole fraction of hydrothermal SO_4^{2-} in the barite, which ranges from 0.1 and 0.9 (Ohmoto et al., 1983).

Precipitation of anhydrite during fluid mixing may occur much like that of barite: by utilizing both hydrothermal and seawater components. For anhydrite, however, local seawater may be an important source for Ca^{2+} as well as SO_4^{2-} because normal seawater contains $\sim 10^{-2}$ *m* of Ca^{2+} (Table 2). A more important difference between anhydrite and barite is that anhydrite, because of its retrograde solubility, may dissolve in the fluid mixtures at temperatures below $\sim$ 150°C (Fig. 5), or in normal seawater during and after settling on the seafloor. This is the reason why anhydrite is found in young chimneys but not in old chimneys on modern-day mid-ocean ridges (e.g., Graham et al., 1988), and why anhydrite is rare within the massive sulfide bodies of VMSDs. Although the anhydrite formed on the seafloor is eventually dissolved by the overlying

Table 2
Chemical compositions of seawater and selected submarine hydrothermal fluids (concentrations of elements in mmol/kg H_2O)

	Seawater	Kuroko	EPR 21°N	Guaymas	Juan de Fuca	Atlantis II	Danakil
T (°C)	15	200–350	270–355	260–315	220–290	56	> 108
pH	8.1	4.7–4.2	3.8–3.3	5.9	3.2	na	< 3.0
Na	468	420–740	430–510	480–510	660–800	5200–5400	6300–7400
K	10	30–140	23–26	33–49	37–52	64–100	80–180
Mg	53	5–30	0	0	0	38–40	70–10000
Ca	10	10–110	12–21	29–42	77–96	170–180	49–240
Fe	0	0.01–1	0.75–2.4	0.02–0.18	10–19	1.5–2.0	150–200
Mn	0	na	0.8–1.0	0.13–0.24	2.6–4.5	1.7–2.0	4.5–11
Cu	0	0.002–0.08	0.01–0.04	< 0.001	< 0.002	na	na
Zn	0	0.1–6	0.04–0.1	0.001–0.04	< 0.6–0.9	na	na
Ba	0	0.01–0.3	> 0.01	> 0.05	na	na	na
Cl	545	490–1100	490–580	580–640	900–1090	5900–6200	7400–15000
ΣSO_4^{2-}	28	0.3–30	0–0.6	0–0.1	0	12–14	12–110
CO_2(aq)	2	50–350	5.7	na	3.9–4.5	na	na
H_2S(aq)	0	0.05–25	6.6–8.4	3.8–6.0	3.0–4.4	na	0.04
SiO_2(aq)	0	4–13	16–20	9–14	23	na	0.8–7

Seawater: Holland (1978). Kuroko ore-forming fluids: Pisutha-Arnond and Ohmoto (1983), Ohmoto et al. (1983); Fe values recalculated using the pyrite solubility data of Ohmoto et al. (1993). EPR, Guaymas Basins, Southern Juan de Fuca: Von Damm (1990). Atlantis II Deep and Danakil Deep of the Red Sea: Lloyd et al. (1976).

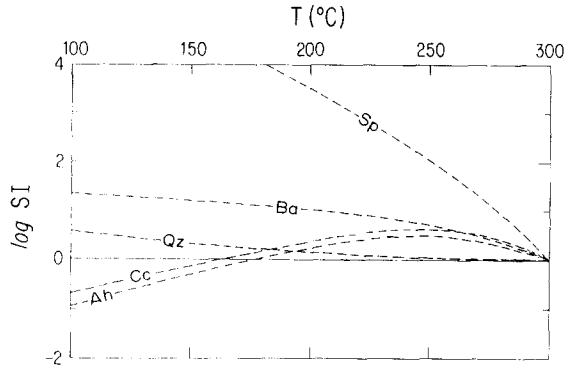

Fig. 5. Calculated changes in the saturation indices (*SI* = activity products of aqueous species in solution/equilibrium activity products of aqueous species) during mixing of a 300°C Kuroko fluid with 0°C seawater. *Sp* = sphalerite, *Ba* = barite, *Qz* = quartz, *Cc* = calcite, *Ah* = anhydite. Modified from Ohmoto et al. (1983).

seawater, anhydrite layers may act as a thermal blanket and may play an important role in the growth of a massive sulfide body as suggested by Eldridge et al. (1983) and Campbell et al. (1984). The anhydrite formed beneath the seafloor, such as the anhydrite body occurring beneath the peripheral parts of the massive sulfide ore (see Fig. 1), may be protected from cold seawater and preserved.

3.3.2. Quartz

Most hydrothermal fluids, particularly those developed in rock sequences dominated by felsic igneous rocks, must be very close to saturation with respect to quartz. Thus, the concentration of silica in hydrothermal fluid must almost always be much higher than that of Ba; for example, ~ 250 ppm of SiO_2 versus ~ 10 ppm of Ba have been estimated for an average Kuroko hydrothermal fluid (Table 2). During mixing of such hydrothermal fluids with cold seawater, the saturation index (or the degree of saturation) for quartz continuously increases during mixing with cold seawater, much like that for barite (Fig. 5). We would expect silica and barium in the hydrothermal fluids to precipitate out quantitatively, and the quartz content in the primitive black ore to be much higher than barite. However, quartz is much less abundant than barite in the primitive black ore. This apparent contradiction can be explained by the difference between the two minerals in the kinetics of nucleation.

Formation of barite (i.e., reactions 1) is an ionic reaction, which takes place almost instantaneously even at room temperature. However, precipitation of quartz from aqueous solutions, in which silica is largely in the form of silicic acid, is a dehydration reaction:

$$H_4SiO_4(aq) \Rightarrow 2H_2O + SiO_2(qtz) \quad (2)$$

Rimstidt and Barnes (1980) have shown experimentally that the rate of reaction (2), for a given mass of fluid, decreases linearly with decreasing surface area of solids (e.g., silicates) on which silica can nucleate, and that the rate decreases also with decreasing temperature. When fluid mixing occurs above the seafloor, the surface area available for the nucleation of quartz is essentially zero, and the cooling rates are very fast; the combined effects, therefore, impede quartz nucleation. This explains why silica is virtually absent in the smokers and sulfide chimneys along the mid-ocean ridges. In fact, the lack of silica in the primitive black ore can be used as an evidence that most of the primitive black ore minerals in the Kuroko deposits crystallized from the fluid mixtures *above* the seafloor.

Precipitation of silica is favored in the stockwork zone, because the highly fractured rocks provide large surface areas for silica to nucleate, and because the cooling rates are slower than in the case of fluid mixing above the seafloor. For the same reasons, thicker massive sulfide ore bodies, particularly those thicker than ~ 10 m, tend to contain appreciable amounts of quartz, particularly toward the base of the ore bodies. This quartz in the massive ores is not a remnant of the primitive black ore, but was added to the massive sulfide ores mostly during the thermal maximum stage, and occurs mostly as fillings of open spaces created during the dissolution of black-ore minerals.

Solomon (pers. commun., 1995) suggests that fracturing of the footwall rocks and also of the massive ores may have been caused by the high velocity of hydrothermal fluids (i.e., hydraulic fracturing), and that some quartz may have precipitated because of the pressure drop on fracturing.

Consideration of the kinetics of silica precipitation also leads to the suggestion that the ferruginous chert layers (silica + hematite + barite) that occurs

above the massive sulfide ores in many VMSDs were formed by mixing of hydrothermal fluids with cold seawater mostly *within* unconsolidated sediments, rather than by mixing of fluids above the seafloor; that is, they formed during the early diagenesis of the sediments rather than being truly syngenetic. Large surface areas provided by fine-grained tuffs and mudstones would have enhanced the precipitation of silica from solution.

3.3.3. Carbonates

Carbonate minerals are unlikely to precipitate during simple cooling of fluids or cooling caused by rapid mixing of cold seawater (see Fig. 5), which explains why carbonate minerals are not common in the primitive black ore. However, some black ores that grew in unconsolidated mudstones, such as the Matsuki deposits in the Hokuroku district, contain some calcite. Such calcite may have formed because the CO_2 content of the fluids increased locally through thermal decomposition by hydrothermal fluids of organic matter in the mudstones:

$$2\text{``}CH_2O\text{''}(s) \Rightarrow CO_2(aq) + CH_4(aq) \quad (3)$$

$$Ca^{2+} + H_2O(l) + CO_2(aq) \Rightarrow CaCO_3(s) + 2H^+ \quad (4)$$

where ``CH_2O'' represents organic matter. In fact, Ohmoto et al. (1983) have found that the $\delta^{13}C$ values of calcites in the Matsuki ore bodies are around $-5‰$, which lies between the $\delta^{13}C$ values of organic carbon in the sediments (-26 to $-22‰$) and normal marine limestone ($\sim 0‰$).

3.3.4. Sphalerite and galena

Mixing of hydrothermal fluid with cold seawater is a very effective mechanism for precipitation of sphalerite and galena (and tetrahedrite), if the hydrothermal fluids contained sufficient amounts of both H_2S and the heavy metals. The saturation indices for these minerals increase continuously with increasing proportions of cold seawater in the mixtures (Fig. 5), primarily because the solubility products for these sulfides decrease rapidly with decreasing temperature; the effect of pH change during fluid mixing is minor (Ohmoto et al., 1983). For example, 20 percent mixing of seawater ($T = 0°C$ and pH = 8.1) into a 300°C fluid (pH = 4.5) causes a 60°C drop in the ore-fluid temperature and only about 0.1 unit increase in the pH; during this mixing, the saturation indices for sphalerite and galena increase by more than two orders of magnitude (Fig. 5). The difference in fluid inclusion filling temperatures between sphalerite in the stockwork ore and that in the primitive black ore is less than 60°C (Pisutha-Arnond and Ohmoto, 1983); this, together with the data in Fig. 5, indicates that the concentration of Zn in the Kuroko ore-forming fluids (Table 2) was within two orders of the saturation values.

Mixing of hot fluids with cold seawater does not always leads to *co-precipitation* of sulfides. Whether one or multiple mineral phases precipitate during fluid mixing depends largely on the $\Sigma metal/H_2S$ molal ratio in the hydrothermal fluid. If this ratio was much larger than 1 (i.e., H_2S deficient) only one sulfide mineral phase, the one which is closest to saturation and also easiest to nucleate, may precipitate; this may create a monominerallic ore. On the other hand, if the $\Sigma metal/H_2S$ ratio was much less than 1 (i.e., H_2S sufficient), more than one sulfide phases may co-precipitate, and form a polymetallic ore. The $\Sigma metal/H_2S$ ratio of hydrothermal fluids appears to be controlled largely by the thermal and compositional (rock type) structures of the plumbing systems. For fluids developed in dominantly felsic volcanic terrains, the ratio generally becomes larger than 1 at temperatures $< \sim 150°C$, but less than 1 at $T > \sim 200°C$ (Ohmoto et al., 1983; Ohmoto, 1986b). This explains why a monomineralic galena layer is developed at the very top part of the black ore zone in some VMSDs; it was formed when the temperature of discharging fluids decreased to $< 150°C$ during the waning stage.

3.3.5. Fe-bearing minerals

The common Fe-bearing minerals that may precipitate during mixing of hot hydrothermal fluid and cold seawater are hematite (goethite), pyrrhotite, and pyrite: magnetite is less common. Which of these Fe-bearing phases precipitates from the fluid mixtures depends largely on: (1) the initial concentrations of ΣFe, H_2S and H_2 in the hydrothermal fluids; and (2) the relative rates of decrease in the concentration of these components during fluid mixing and mineral precipitation, which are determined

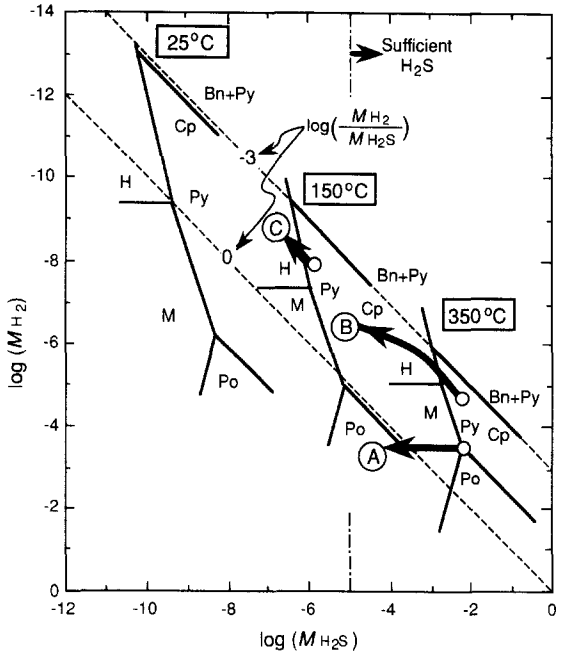

Fig. 6. Stability relations of Cu–Fe–S–O minerals as a function of temperature and the concentrations of aqueous H_2 and H_2S. *Po* = pyrrhotite, *Py* = pyrite, *M* = magnetite, *H* = hematite, *Cp* = chalcopyrite, *Bn* = bornite. Conversion of the fugacity values to the molal concentration values of H_2 and H_2S was made using the solubility data by Drummond (1981) of these gases in 1 *m* NaCl solutions. Thermodynamic data of other reactions are from Ohmoto et al. (1983) and Drummond (1981). *A*, *B* and *C* refer to the three pathways during cooling (see text).

largely by the depositional environments (e.g., within or outside ore mounds).

The initial concentrations of ΣFe, H_2S and H_2 in natural hydrothermal fluids are typically buffered by pyrite + Fe-bearing silicates (e.g., biotite, chlorite) in the plumbing systems, and generally increase with increasing temperatures (Ohmoto, 1986b; Ohmoto and Goldhaber, 1996; see also Fig. 6). For the hydrothermal fluids developed in felsic volcanic terrains, the H_2S content ranges typically between 10^{-7} and 10^{-4} *m* at $T \approx 100$°C, and between 10^{-4} and 10^{-1} *m* at ~ 350°C; the molal ratio of H_2S/H_2 falls typically between 1 to 10^{-3} (Fig. 6); the ratios of $\Sigma Fe/H_2S$ and $\Sigma Fe/H_2$ may become higher or lower than 1. Variations in the mineralogy of the Fe-bearing phases that may precipitate during fluid mixing probably reflect differences in the initial fluid composition and the depositional environments as summarized below:

Precipitation of pyrrhotite can be simplified as:

$$Fe^{2+} + H_2S(aq) \Rightarrow FeS(s) + 2H^+ \quad (5)$$

The reaction is favored if: (1) the H_2S/H_2 ratio of a hydrothermal fluid was initially in or near the stability field of pyrrhotite (± pyrite ± Fe-silicates), i.e., fluids developed in mafic igneous rocks; and (2) the removal rates of Fe^{2+} and H_2S by the above reaction are faster than the rate of H_2 decrease (see pathway A in Fig. 6), such as during rapid mixing with cold seawater. This is probably the reason why pyrrhotite, rather than pyrite, is the dominant Fe-bearing mineral in the black smokers in the East Pacific Rise at 21° and 13°N (e.g., Haymon and Kastner, 1981). The amount of pyrrhotite precipitating is limited by the smaller of the two, ΣFe and H_2S.

Nucleation of pyrite in submarine hydrothermal deposits may occur through two possible pathways, one via transformation of pyrrhotite, and the other by direct precipitation from solutions. Based on experiments at $T < 100$°C, Schoonen and Barnes (1991) has suggested that the nucleation of pyrite proceeds always through an initial formation of pyrrhotite (and other iron monosulfides), even when the solution was supersaturated with respect to pyrite; the iron monosulfides are subsequently transformed to pyrite through reactions such as:

$$2FeS(s) + 2H^+ \Rightarrow FeS_2(s) + Fe^{2+} + H_2(aq) \quad (7)$$

or:

$$FeS(s) + H_2S(aq) \Rightarrow FeS_2(s) + Fe^{2+} + H_2(aq) \quad (8)$$

However, Graham and Ohmoto (1994) have shown through hydrothermal experiments at $T = 150° - 350$°C that direct nucleation of FeS_2 (pyrite or marcasite) from solutions can occur when the solutions are undersaturated with respect to pyrrhotite. Nucleation and growth of FeS_2 (pyrite or marcasite) crystals can be written as:

$$Fe^{2+} + H_2S_2(aq) \Rightarrow FeS_2(s) + 2H^+ \quad (9)$$

Reaction (9) is also necessary for pyrite to grow continuously on the pyrite that nucleated from pyrrhotite via reaction (7) or (8).

Because the equilibrium concentration of H_2S_2 (and other polysulfide species) in hydrothermal fluids is much less than that of H_2S and/or aqueous sulfates (e.g., Murowchick and Barnes, 1986), for FeS_2 crystals to grow polysulfides must be continuously created *at depositional sites* by oxidation of H_2S and/or reduction of SO_4^{2-}, regardless of whether the fluids were initially in the stability field of pyrrhotite or pyrite (see pathway B in Fig. 6). The possible reactions include:

$$2H_2S(aq) + 1/2\,O_2(aq) \Rightarrow H_2S_2(aq) + H_2O(l) \quad (10)$$

$$2H_2S(aq) \Rightarrow H_2S_2(aq) + H_2(aq) \quad (11)$$

$$7H_2(aq) + 4H^+ + 2SO_4^{2-} \Rightarrow H_2S_2(aq) + 8H_2O \quad (12)$$

and:

$$7H_2S(aq) + 2H^+ + SO_4^{2-} \Rightarrow 4H_2S_2(aq) + 4H_2O \quad (13)$$

If the fluids were initially in the stability field of pyrrhotite, the oxidation reactions (10 or 11) must proceed faster than reaction (5); the cooling rate must be relatively slower than the oxidation rate. Note that for pyrite to nucleate via reactions (7) and (8), a mechanism to remove H_2 (i.e., oxidation) is also required.

In the depositional environments of VMSDs, there are several possible mechanisms that facilitate production of polysulfide from H_2S: (a) mixing of O_2-bearing seawater in warm ore piles; (b) H_2 diffusion into surrounding seawater and rocks; and (c) reaction with previously formed sulfate minerals (i.e., reactions 12 and 13) in ore piles and in the footwalls. The rate of reactions (12) and (13) may be similar to (but not the same as) that of the reaction forming thiosulfate from H_2S and SO_4^{2-}, which has been investigated by Ohmoto and Lasaga (1982). It may require ~ hours at ~ 350°C and ~ years at ~ 150°C to generate sufficient amounts of H_2S_2 from reactions (12) and/or (13). In other words, reactions (12) and (13) may not be important during rapid mixing of H_2S-bearing hot hydrothermal fluids and SO_4^{2-}-bearing seawater, but may become important in environments where a warmer temperature and a steady supply of SO_4^{2-} are maintained for an extended period, such as within anhydrite-(and/or barite-)bearing massive bodies. The availability of mechanisms to promote reactions (10)–(13) may explain why FeS_2, rather than FeS, is the dominant Fe-sulfide in the sulfide–sulfate chimney walls (Graham et al., 1988), and also why pyrite is the dominant sulfide mineral in the lower part of massive sulfide deposits (see Fig. 1).

Precipitation of hematite (or goethite), which may be written as:

$$2Fe^{2+} + 3H_2O(l) \Rightarrow Fe_2O_3(s) + 4H^+ + H_2(aq) \quad (14)$$

requires also an oxidation mechanism. If hydrothermal fluids were low temperature (≤ 150°C) and near the stability fields of pyrite + hematite, they are likely to contain much less H_2S ($< 10^{-4}$ *m*) than Fe ($> 10^{-4}$ *m*) (Fig. 6). Oxidation of such fluids is likely to precipitate more hematite than pyrite (see pathway C in Fig. 6).

3.4. Metasomatic transformation of ore

3.4.1. Recrystallization and selective dissolution of black ore

The fine-grained primitive black-ore minerals that crystallized in the plume at $T > 150$°C may be cooled to ambient temperatures before settling onto the seafloor, and accumulating on the older black ore. The new layer of black ore acts as a thermal blanket for the older black ore, allowing the older ore to be reheated by incoming hydrothermal fluids and recrystallized to coarser-grained black ore (i.e., facies-2 ore). Thus, with increasing thickness of a massive sulfide ore, the ore becomes increasingly coaser-grained toward the bottom of an ore pile.

The hydrothermal fluids, before interacting with the ore pile, were most likely saturated with quartz and pyrite, but undersaturated with respect to other major sulfides (e.g., sphalerite, galena, chalcopyrite) and sulfates (anhydrite and barite); quartz and pyrite are two of the most common minerals in almost all types of country rocks of VMSDs, but the other sulfides and sulfates are not. About one third of footwall rock samples from the sericite–chlorite zone of the Kuroko deposits show loss of Zn and Pb, and another one-third show no loss or gain (Ohmoto et

al., 1983; see also Fig. 13). Such data support the suggestion that the hydrothermal fluids were close to saturation, but undersaturated with respect to most major sulfides before mineralization. Cooling of such fluids near the seafloor probably caused the disseminated sulfide mineralization that was responsible for the increases in the Zn and Pb contents of the other one-third of samples. The solubilities of most black-ore minerals increase with increasing temperatures. Therefore, the later and hotter hydrothermal fluids were probably more capable of dissolving the black-ore minerals.

The rates of dissolution of the black-ore minerals are not the same for all minerals. Microscopic studies (e.g., Eldridge et al., 1983) of the massive ores suggest that the dissolution rates decrease in the order of barite → galena → sphalerite → pyrite. Barite and galena are dissolved almost completely by the time the primitive black ore is converted to the yellow ore; almost all the sphalerite has been dissolved from the massive pyrite ore. Such differential rates of dissolution of the black-ore minerals have resulted in the decreasing trends of Ba/Pb, Pb/Zn, and Zn/Fe ratios downward in a massive ore body (Pavelka, 1984).

The increase in the proportion of pyrite from the black ore to the yellow ore is due not so much to the formation of new pyrite in the yellow ore as to the faster rates of dissolution of other black-ore minerals compared to pyrite. Even some pyrite was dissolved during the conversion of black ore to yellow ore. However, in the massive pyrite ore, new pyrite was added to the older pyrite (see later discussion on "Dissolution of chalcopyrite and formation of massive pyrite ore").

3.4.2. Replacement of black ore minerals by chalcopyrite

The dissolution of barite, sphalerite, and galena by the later hydrothermal fluids is easy to understand, because the hydrothermal fluids were probably undersaturated with these minerals before interaction with the ores. However, the dissolution of pyrite is not, because the fluids were presumably saturated with pyrite even before interaction with the black-ore minerals. This apparent contradiction can be readily explained, if the dissolution of other black-ore minerals was accompanied by the formation of chalcopyrite (i.e., replacement of the black-ore minerals by chalcopyrite); such reactions may have created a local environment that was hostile to pyrite.

For example, dissolution of sphalerite (and galena) consumes H^+ and generates H_2S locally:

$$ZnS(s) + 2H^+ \Rightarrow H_2S(aq) + Zn^{2+} \quad (15)$$

which is favored by heating. This may cause precipitation of chalcopyrite from fluids that were initially undersaturated with chalcopyrite by driving the following reaction forward:

$$Cu^- + Fe^{2+} + 2H_2S(aq) \Rightarrow CuFeS_2(s) + 3H^+ + 1/2\,H_2(aq) \quad (16)$$

Theoretically, chalcopyrite can precipitate directly from hydrothermal solutions via reaction (16). However, the probability for three molecules [Cu^+-chloride complex, Fe^{2+}-chloride complex, and $H_2S(aq)$] to collide and form nucleus of chalcopyrite is likely to be much less than that for two molecules [e.g., Zn^{2+}-chloride complex and $H_2S(aq)$] to cause nucleation of sphalerite or galena. This is probably the main reason why the primary precipitation of chalcopyrite from hydrothermal solution is not as common as sphalerite and galena.

The combination of reactions (15) and (16) is an overall reaction for replacement of sphalerite (and galena) by chalcopyrite:

$$2ZnS(s) + H^+ + Cu^+ + Fe^{2+} \Rightarrow CuFeS_2(s) + 2Zn^{2+} + 1/2\,H_2(aq) \quad (17)$$

The increase in the activity of H_2 caused by reaction (17) may drive the following reaction of dissolution of pyrite forward:

$$FeS_2(s) + 2H^+ + H_2(aq) \Rightarrow Fe^{2+} + 2H_2S(aq) \quad (18)$$

The combination of reactions (16) and (18) is an overall reaction of replacement of pyrite by chalcopyrite:

$$Cu^+ + FeS_2(s) + 1/2\,H_2(aq) \Rightarrow CuFeS_2(s) + H^+ \quad (19)$$

Reaction (17) indicates that replacement of sphalerite (and galena) by chalcopyrite may continue as long as there is an effective mechanism to consume H_2 locally; while reaction (19) indicates that pyrite

may be replaced by chalcopyrite when there is an effective mechanism to generate H_2 locally. That is, the replacement of the black-ore minerals by chalcopyrite may occur most effectively where sphalerite (and/or galena) and pyrite are both present.

An overall reaction for the replacement of sphalerite (or galena) and pyrite by chalcopyrite is the combination of reactions (17) and (19).

$$2ZnS(s) + FeS_2(s) + 2Cu^+ + Fe^{2+} \Rightarrow 2CuFeS_2(s) + 2Zn^{2+} \quad (20)$$

Reaction (20) indicates that 2 moles of sphalerite (and/or galena) and 1 mole of pyrite may be converted to 2 moles of chalcopyrite during the interaction with Cu- and Fe-bearing hydrothermal solutions. The stoichiometry of the reaction implies that sphalerite (and/or galena) is consumed at a faster rate than pyrite, and that the volume of new minerals (chalcopyrite) is less than that of the older minerals (sphalerite + galena + pyrite). This explains why, as the primitive black ore is continuously converted to yellow ore, the Zn/Fe and Pb/Fe ratios of massive ores decreases drastically with increasing Cu content, and the porosity of ores also increases. The yellow-ore with very high porosity disintegrates readily, and is called "sandy yellow ore". The open spaces created by reaction (20) may partially be filled by later generation of quartz, explaining why vugs containing euhedral crystals of quartz and chalcopyrite are more abundant in the yellow ore than in the black ore.

The formational mechanisms for chalcopyrite in other types of ore deposits, such as the SHMSDs and MVT, were probably similar to those in VMSDs. For example, the Cu-rich massive sulfide ores in the Mt. Isa deposits may have formed by replacement of sphalerite–galena–pyrite rich ores via reaction (20).

3.4.3. Dissolution of chalcopyrite and formation of massive pyrite ore

The above reactions (15)–(20) suggest that the formation of chalcopyrite and dissolution of pyrite may cease once all the sphalerite and galena in the yellow ore are totally consumed. Thereafter, chalcopyrite in the yellow ore starts to be dissolved, because the discharging hydrothermal fluids were probably undersaturated with respect to chalcopyrite. Some chalcopyrite may be dissolved through the reverse reaction of (16) or (19), or their combination:

$$2CuFeS_2(s) + 4H^+ \Rightarrow 2Cu^+ + Fe^{2+} + FeS_2(s) + 2H_2S(aq) \quad (21)$$

These reactions, (21) and reversal of (19), produce new pyrite at the expense of the earlier chalcopyrite. Furthermore, if fluids are allowed to cool slowly and H_2 is allowed to be removed slowly (see previous section of "Fe-bearing minerals"), additional pyrite may be formed by the back reaction of (18).

The above suggested sequence of chemical reactions, which leads to the sequential conversion of black ore → yellow ore → pyrite ore, is supported by the fact that in the massive pyrite ore, virtually all sphalerite and galena had been dissolved out, and at least two types of pyrite are present: (1) the remnant of the black-ore pyrite, which were initially boytroidal or framboidal forms; and (2) coaser-grained, euhedral pyrite, which appears to fill the open spaces created by dissolution of sphalerite, galena, chalcopyrite, and sulfate minerals (see Eldridge et al., 1983).

3.5. Chemical evolution of a growing massive ore body

It would be easy to recognize that the Cu dissolved from the massive pyrite ore by reaction (21) would be carried outward by the hydrothermal fluids where it may reprecipitate as chalcopyrite through reactions with unreacted black ore minerals through reactions (15)–(17). Some of the Zn, Pb, Fe, Ca and Ba which were dissolved from the black ore may reprecipitate in the exterior of an ore body when the hydrothermal fluids mix with cold seawater. *If* all the metals and H_2S in the hydrothermal fluids reprecipitate during mixing with cold seawater, and settle on the ore body, and *if* the metal chemistry of the discharging hydrothermal fluids remained constant during the growth of an ore body, then, the metal ratios among Zn, Pb, Fe, Ca and Ba of the bulk ore body would remain the same, even though the ore-body size may increase and the metal zoning, black ore — yellow ore — pyrite ore, within the ore body may become more pronounced.

However, only a small fraction of metals in hy-

drothermal fluids appears to precipitate at the site of mixing with cold seawater. For example, along the East Pacific Rise, only ~ 1 to ~ 10% of the metals appear to be fixed in the chimneys, and the remaining metals are dispersed in the overlying seawater (e.g., Edmond et al., 1979). Furthermore, during the thermal waxing stage, the higher-temperature fluids generally contain higher ratios of Cu/Zn and Cu/Pb than the earlier, colder fluids (see later section). Therefore, the combined effect of partial reprecipitation of metals and changing fluid chemistry cause the metal ratios of the bulk ore body to continuously change during the maturation of an ore body. A typical sequence, with increasing degree of maturity or with an increasing ratio of height/width of an ore body, is Pb- and Ba-rich black-ore type → Zn-rich black-ore type → yellow-ore type → pyrite-ore type (see Fig. 4). According to this model, the large pyrite-rich VMSDs in the Iberian pyrite belt represent the most mature example of this deposit type of VMSDs.

3.6. Precipitation of precious metals in VMSDs

3.6.1. Silver

Silver occurs in the Kuroko ores mostly as trace to major constituents in a variety of sulfosalts, such as tetrahedrite, tennantite, and polybasite (e.g., Ishihara, 1974). Minor amounts of silver occur also in galena, acanthite and electrum. The common occurrence of Ag as sulfosalts and sulfides in VMSDs, rather than electrum, probably reflects the fact that the silver is transported in hydrothermal solutions as Ag^+-complexes (with either chloride and/or bisulfide as the complexing ligand), and precipitation of Ag^+-bearing minerals, such as:

$$2Ag^+ + H_2S(aq) \Rightarrow Ag_2S(s) + 2H^+ \quad (22)$$

is much easier than that of Ag°-bearing minerals (e.g., Ag-rich electrum):

$$Ag^+ + 1/2\,H_2(aq) \Rightarrow Ag(s) + H^+ \quad (23)$$

because reaction (23) requires a reducing (i.e., high H_2) condition.

In contrast to a popular belief that Ag^+ and Pb^{2+} behaves similarly, the Ag/Pb ratio varies greatly within an ore body, and between deposits. However, the Ag/Zn ratios are much more uniform at ~ 1/1000 in weight ratio in most VMSDs (see Table 1), suggesting that Ag^+ and Zn^{2+} may behave similarly in hydrothermal fluids, during mixing of hydrothermal fluids and cold seawater, and during interaction between ores and fluids.

3.6.2. Gold

Although the gold contents in the black ore and barite-rich ores tend to be higher than that in the yellow ore and massive-pyrite ore, gold rarely is co-precipitated with sphalerite, galena, barite and other black-ore minerals. Gold (as electrum) occurs primarily in the fractures and grain boundaries of the black ore minerals, commonly together with Cu-bearing minerals, suggesting that the formation of gold took place during the thermal maximum stage. The Au/Ag ratios are extremely variable within an ore body, ranging from less than 1/1000 to ~ 1/10: the average Au/Ag ratio for all VMSDs is about 1/60 (Table 1).

Experimental study by Hayashi and Ohmoto (1991) on the solubility of gold in NaCl- and H_2S-bearing hydrothermal solutions suggests that gold in most hydrothermal solutions is transported as bisulfide complexes. The dominant precipitation reaction at pH < ~ 6 is:

$$HAu(HS)_2 + 1/2\,H_2(aq) \Rightarrow Au(s) + 2H_2S(aq) \quad (24)$$

The equilibrium constant for reaction (24) is essentially constant in a temperature range of 250°–350°C. Therefore, simple cooling is not an effective mechanism to precipitate gold. Normal bottom seawater contains ~ $10^{-3.5}$ *m* dissolved O_2. During the mixing of hydrothermal fluids with oxygenated seawater, the increasing O_2 content in the fluid mixtures is likely to decrease the H_2 content at a faster rate than the H_2S content, impeding gold precipitation (Hayashi and Ohmoto, 1991). This explains the rare occurrence of gold in the primitive black ore.

The most effective mechanism to precipitate gold is provided when the H_2S content of fluids is decreased and the H_2 content increased. Such a mechanism is provided when chalcopyrite precipitates from the solution by reaction such as (17). This explains the observed association of Au and Cu in VMSDs.

3.7. Mechanical processes of ore-brecciation and resedimentation

Mechanical disintegration (including chimney collapse), transportation, and redeposition of mineral grains and ore fragments appear to have been very common throughout the entire growth history of massive ores. For example, most of the ore samples examined by Eldridge et al. (1983), including those from some Archean VMSDs, exhibit some clastic textures. Post-hydrothermal slumping of ore bodies also created variations in large-scale features, such as the sharp, rather than diffuse and gradational, boundaries between the different ore types (e.g., between the yellow and black ores), ore bodies with a reverse zoning (e.g., ores of black-ore fragments lying underneath the ores composed of yellow-ore fragments), and massive ore bodies that are detached from the stockwork zone.

4. Processes of seawater–rock interaction (evolution of ore-forming fluids)

Obvious questions that follow the above discussions on the chemical processes of ore growth concern the chemistry of the ore-forming fluids, especially the concentrations of the heavy metals and H_2S, the origin of the fluid components, and the processes that controlled the fluid chemistry.

4.1. Isotopic and chemical compositions of fluids and rocks

4.1.1. Fluids

The salinities of primary fluid inclusions in the Kuroko ores, as indicated by their freezing temperatures, range from ~2 to ~8 wt% NaCl equivalent, but are mostly around 4 wt% (Pisutha-Arnond and Ohmoto, 1983). The similarity in the salinity between the Kuroko fluids and normal seawater, and the lack of correlation between the salinity and temperature are some of the evidences for the seawater origin for the Kuroko ore-forming fluids. The salinities of the hydrothermal fluids associated with the black smokers on mid ocean ridges (MOR) are quite similar to those of the Kuroko fluids, but those in the Red Sea are much more saline (Table 2).

The concentrations of major elements and CO_2 in the Kuroko fluids (Table 2) were estimated from the analyses of extracted inclusion fluids, most of which are associated with the thermal maximum (Cu-mineralization) stage of hydrothermal activity. Some of the important characteristics of the major element chemistry of the Kuroko hydrothermal fluids and the MOR fluids are increases from the seawater values in K and Ca, but a decrease in Mg relative to seawater (Table 2).

The suggestion that the Kuroko ore-forming fluids were merely seawater that acquired heat, metals and H_2S during deep circulation through the underlying volcanic rocks was first proposed by Ohmoto et al. (1970) from the results of a few analyses of hydrogen and oxygen isotopic compositions of fluid inclusions in some Kuroko minerals: the δD and $\delta^{18}O$ values, as well as the salinity values, were found to be very similar to those of normal seawater. More extensive studies conducted by later investigators (Ohmoto and Rye, 1974; Hattori and Sakai, 1979; Pisutha-Arnond and Ohmoto, 1983; Tsutsumi and Ohmoto, 1983) have enlarged the δD–$\delta^{18}O$ field of the Kuroko ore-forming fluids considerably: $\delta D = -20$ to $+20‰$ and $\delta^{18}O = -8$ to $+4‰$ (Fig. 7).

An interesting feature of Kuroko ore-forming fluids is that the change with time in the $\delta^{18}O$ value of hydrothermal fluids parallels fluid temperatures. The $\delta^{18}O$ increased from around $-8‰$ at ~100°C during Period I mineralization to around $+2‰$ at ~

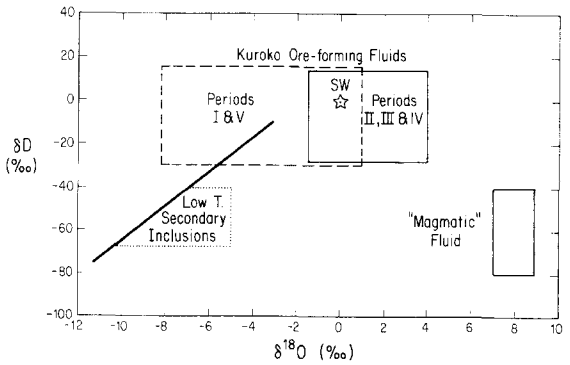

Fig. 7. δD–$\delta^{18}O$ relationship of the Kuroko ore ore-forming fluids and of low temperature secondary inclusions. The temperatures of ore-forming fluids were ~100– ~200°C for periods I and V, and ~200– ~400°C for Periods II, III and IV. Modified from Pisutha-Arnond and Ohmoto (1983).

350°C during the waxing stage (Period III) of hydrothermal activity, and decreased back to around $-10‰$ at ~ 100°C (Period V); during most of the mineralization periods (i.e., Periods II–IV), the $\delta^{18}O$ values remained within $\pm 2‰$ of 0‰. A simple interpretation of such data is much like the one suggested by Ohmoto and Rye (1974) and Hattori and Sakai (1979), and assumes mixing of three types of water: meteoric water with the $\delta^{18}O$ values $< 0‰$, seawater of $\sim 0‰$, and magmatic water of $\sim +8‰$. The paleogeographic setting of the Kuroko deposits suggests, however, that a contribution of meteoric water was extremely unlikely for the mineralization sites were under $> \sim 2000$ m of seawater and with the nearest land mass was located more than 50 km away (Ohmoto, 1983; Guber and Merrill, 1983). Contributions of meteoric water were recognized for the secondary inclusions (Fig. 7), which appear to have trapped in the Kuroko ore minerals after the deposits were uplifted from a submarine to a subaerial environment.

The δD and $\delta^{18}O$ values for hydrothermal fluids responsible for many other VMSDs fall in the same range as Period II–IV Kuroko ore-forming fluids. Examples include the Cretaceous Cyprus deposits (Heaton and Spooner, 1977), the Rio Tinto, the Aljustrel, Salgardinho and the Chança deposits of the Iberian Pyrite Belt (Munha et al., 1986), and the Proterozoic Crandon deposit (Munha et al., 1986). Where the δD values have not been determined, the $\delta^{18}O_{H2O}$ values fall in the range as Period II–IV Kuroko ore-forming fluids, ~ -2 to $\sim +4‰$, at the Corbit, the Ansil, the Amulet, the Norbec, the Horne, and the Mobrun deposits of Archean ages in the Noranda district (Fig. 8), the Mattagami deposit (Costa et al., 1983) and the South Bay deposit (Urabe et al., 1983) of Archean ages. The δD and $\delta^{18}O$ values for recent submarine hydrothermal fluids, such as in the Red Sea and in the East Pacific Rise, are not as large as those for the Kuroko fluids, but are also similar to those of normal seawater (see Ohmoto, 1986a for a review). These data suggest that seawater has been the major (or sole) component in most submarine hydrothermal fluids.

The "magmatic component" in the ore-forming fluids for the Kuroko and many other VMSDs, especially during the high-temperature stage, cannot be dismissed, because the $\delta^{18}O_{H2O}$ values are as high

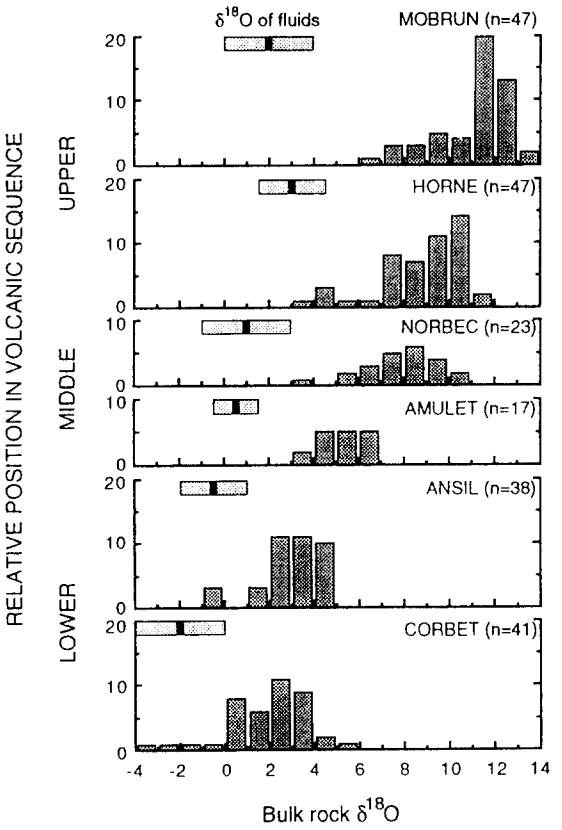

Fig. 8. Frequency distribution of bulk, altered rock $\delta^{18}O$ values with estimated ranges of hydrothermal fluids $\delta^{18}O$ values for individual volcanogenic massive sulfide deposits in the Noranda district, Canada. From Hoy (1993).

as $+4‰$. Li and Manuel (1994) has recognized that the abundance ratios of Ne, Ar and Xe (present probably in fluid inclusions) in some Kuroko ores are similar to those in glasses of submarine volcanic rocks, and suggested that about 75% of these gases were of magmatic origin and about 25% of seawater origin. However, it is difficult to distinguish whether these gases in the Kuroko ores represent direct contributions of magmatic gases or those leached from volcanic rocks by seawater. Furthur more, the origin of H_2O and that of some volatile components, such as Ne (and possibly SO_2), need not have been the same. This is best illustrated by the fact that, in most modern submarine hydrothermal systems, the δD and $\delta^{18}O_{H2O}$ values of high temperature vent fluids are essentially the same as those of seawater, while the helium isotopic ratios and other noble gases

show magmatic values (e.g., Craig et al., 1980; Melivat et al., 1987; Evans et al., 1988; Kennedy, 1988). The model which best fits the thermal and $\delta^{18}O$ history of the fluids and country rocks is the one postulating a continuous interaction of seawater and volcanic rocks; no meteoric or magmatic water is required (see later sections for more discussion).

There are several examples where the $\delta^{18}O$ values of hydrothermal fluids involved in massive sulfide formation are greater than +4‰: $\delta D = -10$ to +50‰ and $\delta^{18}O = +6$ to +14‰ at the Cretaceous Raul deposit (Ripley and Ohmoto, 1977); $\delta D = -20$ to −40‰ and $\delta^{18}O = +5$ to +7‰ at the Silurian Blue Hill deposits (Munha et al., 1986), and $\delta^{18}O = +6$ to +9‰ at the Archean Kidd Creek deposits (Beaty and Taylor, 1982). Magmatic fluid may have been an important component in the hydrothermal fluid at the Blue Hill deposits (Munha et al., 1986). However, the δD and $\delta^{18}O$ values of hydrothermal fluid at the Raul deposits can be better explained by processes of interaction between evaporated seawater and rock (Ripley and Ohmoto, 1977).

4.1.2. Rocks

The alteration zoning around VMSDs has been interpreted by most previous investigators with a single-stage model, in which high-temperature hydrothermal fluids migrated outward from the center of discharge and were gradually cooled by the wall rocks and converted the fresh volcanic rocks to a sericite–chlorite assemblage at high temperatures, montmorillonite at intermediate temperatures, and finally to zeolites under the coolest conditions. However, paragenetic studies of alteration minerals (e.g., Pisutha-Arnond and Ohmoto, 1983) suggest that the alteration was a product of intensifying hydrothermal activity, because the low temperature assemblage was formed first, and was subsequently converted to higher-temperature assemblages by interaction with the later, hotter hydrothermal fluids. The suggested temporal sequence of alteration is: zeolite-I (Mg,Na-type montmorillonite + clinoptilolite + mordenite + saponite + low cristobalite) → zeolite-II (analcime + calcite + illite + quartz) → montmorillonite (characterized by Mg,Ca-type montmorillonite) → transitional mixed-layer clay minerals (illite–montmorillonite mixed layer minerals) → sericite/chlorite (sericite + Mg-chlorite).

The alteration zoning around many other massive sulfide deposits occurring in felsic volcanics are similar to that of the Kuroko deposit. However, in many Archean VMSDs in the Abitibi district, Mg-rich chlorite has been converted to Fe-rich chlorite in the central zone (e.g., Urabe et al., 1983)

Some of the important trends in the major element chemistry of whole rocks around the Kuroko deposits, summarized in Fig. 10, are: (1) a significant increase in the H_2O content in the zeolite-facies rocks, from ~ 1 wt% in "unaltered" rocks to ~ 10 wt%; (2) a subsequent decrease in the H_2O content with increasing grade of hydrothermal alteration, down to ~ 3 wt% in the sericite–chlorite zone; (3) an increasing trend in the MgO content with increasing grades of alteration, from ~ 0.1 wt% in "unaltered" rocks to ~ 0.5 wt% in zeolite facies, and ~ 4 wt% in the sericite–chlorite zone; (4) an increase in the K content in the sericite/chlorite zone; and (5) decreases in the Ca, Sr and Ba contents in the sericite/chlorite zone.

An excellent correlation has been found between the alteration mineral assemblages and the $\delta^{18}O$ values of wall rocks around the Kuroko deposits: +13 to +23‰ for the zeolite facies, +7 to +17‰ for the montmorillonite facies, and +4 to +8‰ for the sericite–chlorite facies (Figs. 9 and 10). The least altered volcanic rocks in the district have $\delta^{18}O$

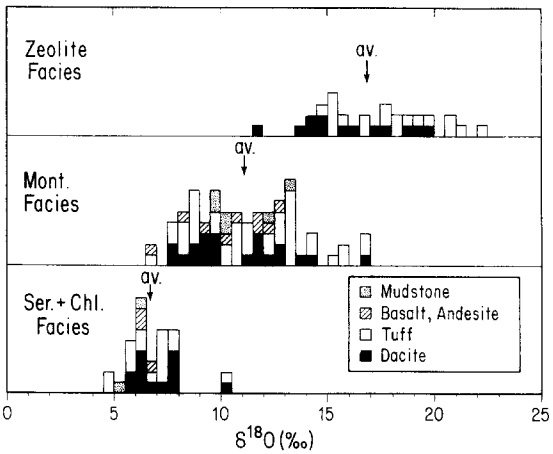

Fig. 9. Frequency distribution of the whole-rock $\delta^{18}O$ values of volcanic rocks around the Kuroko deposits, grouped by alteration zones. Each square represents one rock sample. *mon.* = montmorillonite, *ser.* = sericite, *chl.* = chlorite, *av.* = average. From Green et al. (1983).

values around +6‰. Decreases in the $\delta^{18}O$ values to ~ −4‰ and increases to ~ +14‰ have been found in the altered rocks around VMSDs in the Noranda district (Fig. 8). The strong enrichment in ^{18}O, with the $\delta^{18}O$ values of up to ~ +25‰, has also been found among submarine basalts that have been altered at low temperatures (e.g., Muehlenbachs, 1980). The trend of decreasing $\delta^{18}O$ values from > 10‰ in the peripheral zone to ~ 5‰ in the ore zone has also been found around many VMSDs (see Franklin et al., 1981, for a compilation of data).

The δD values of whole rocks in the alteration zones around VMSDs range from ~ −35 to ~ −100‰ (Hattori and Muehlenbachs, 1980; Green et al., 1983), but no obvious correlation has been found between the δD values and the alteration assemblages.

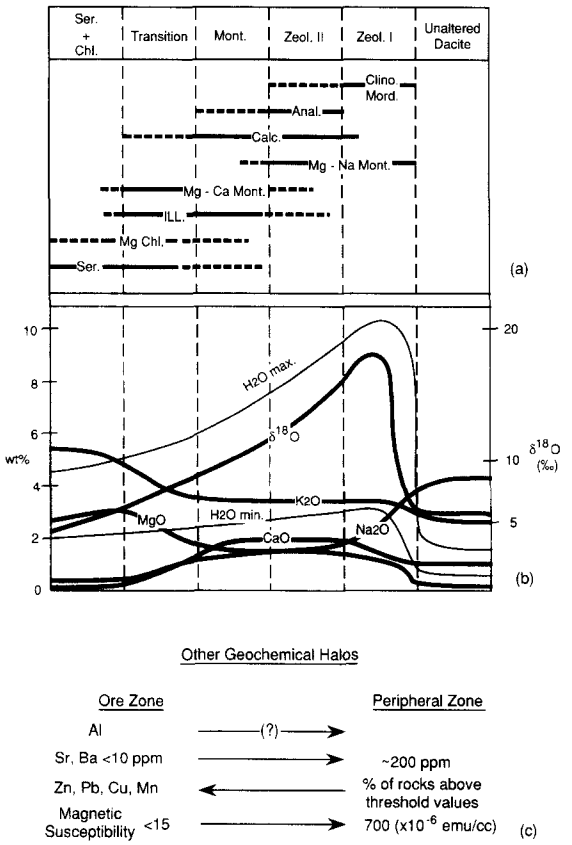

Fig. 10. Mineralogical and chemical characteristics of alteration zones around the Kuroko deposits. (a) mineral assemblages, (b) average major element contents, and (c) other geochemical haloes. *ser.* = sericite, *chl.* = chlorite, *mont.* = monmorillonite, *zeol.* = zeolite, *clino.* = clinoptilolite, *mord.* = mordenite, *anal.* = analcime, *calc.* = calcite, *ill.* = illite. Arrows in (c) indicate directions of increase in the concentrations. Data are from Date et al. (1983), Hashiguchi et al. (1983) and Green et al. (1983).

4.2. Alteration processes

The above characteristics of the ore-forming fluids and the wall rocks associated with the Kuroko deposits can be explained best by a model of seawater–rock interaction in a dynamic system (Fig. 11) where the following conditions are satisfied: (1) the system is open to the overlying seawater, so that fresh seawater is continuously supplied to the system in the low-temperature regions, and continuously removed from the high-temperature regions; (2) the system is thermally intensifying (i.e., increasing temperature with time); (3) the duration of time for a given packet of seawater to circulate through the rock system is much shorter than the life time of the hydrothermal activity in the system (e.g., ~ 10 to ~ 100 years versus ~ 100 to ~ 10 000 years); (4) at any given time and space, for a given packet of water the system is rock-dominated (e.g., w/r mass ratio = ~ 0.02 because the intrinsic water/rock ratio is a measure of the porosity of the rock: see Ohmoto, 1986a); (5) over the life time of the hydrothermal activity, the *integrated* water/rock ratios for any part or the whole of the system may become water-dominated (i.e., w/r > 1). The conditions (3)–(5) imply that the isotopic and chemical compositions of fluids at any time were buffered by the "fresh" minerals in the igneous rocks and/or by the alteration minerals that formed during the earlier and lower-temperature stage as the fluids migrate, while those of rocks reflect the seawater–rock interaction over the life time of the hydrothermal activity.

The principal types of reactions that take place during fluid–rock interaction are hydration and dehydration, cation exchange, precipitation and dissolution, and redox reactions. The importance of these reactions in controlling the isotopic and chemical characteristics of rocks and fluids at different stages of hydrothermal activity are discussed below except for redox reactions which will be discussed in a later section on "Leaching of sulfur from rocks and reduction of seawater sulfate".

4.2.1. Zeolite-I stage

Before the intrusion of a local heat source into the footwall rocks to initiate local convection of seawater, the rocks may interact with pore fluids (seawater) at relatively low temperatures, $< \sim 50°C$ (Fig. 11A). An important reaction during this stage is the hydration of volcanic glass to form zeolite and smectite:

$$H_2O + \text{glass} \Rightarrow \text{zeolite and smectite} \quad (25)$$

This reaction increases the H_2O content (up to ~ 10 wt%) and $\delta^{18}O$ value (up to $+25‰$), and may possibly decrease the δD value of the initial rock (to $\sim -70‰$). The consumption of H_2O in the reaction may cause an increase in the salinity and δD value and a decrease in the $\delta^{18}O$ value of the pore fluids (seawater). For example, an increase in salinity of the seawater pore fluid from ~ 3.5 wt% to ~ 6 wt% may be accompanied by changes in the δD values to $+30‰$ and the $\delta^{18}O$ values to $-15‰$ (Pisutha-Arnond and Ohmoto, 1983). In fact, a trend of decreasing $\delta^{18}O$ values (down to $\sim -8‰$) of the pore fluids with increasing depths from the seafloor has been recognized at many sites of the Deep Sea Drilling Projects (Lawrence and Gieske, 1981)

Cation exchange reactions between pore fluids and smectite (and/or zeolite), such as:

$$Ca - \text{smectite} + Mg^{2+} \Rightarrow Mg - \text{smectite} + Ca^{2+} \quad (26)$$

are probably the principal mechanism for fixation of seawater-Mg in submarine volcanic rocks (Mizukami and Ohmoto, 1983). Some of the Ca released from the rock is used to form gypsum or anhydrite:

$$Ca^{2+} + SO_4^{2-} \Rightarrow CaSO_4(s) \quad (27)$$

Without additional Ca from rock, seawater must be heated to above $\sim 150°C$ to form $CaSO_4$(Mottl and Holland, 1978), but Mizukami and Ohmoto (1983) have shown that gypsum or anhydrite are formed at any temperature, even at $\sim 0°C$, during the interaction of seawater with volcanic rocks (especially tuffs) through a combination of reactions (26) and (27).

Some of the Ca released by reaction (26) may

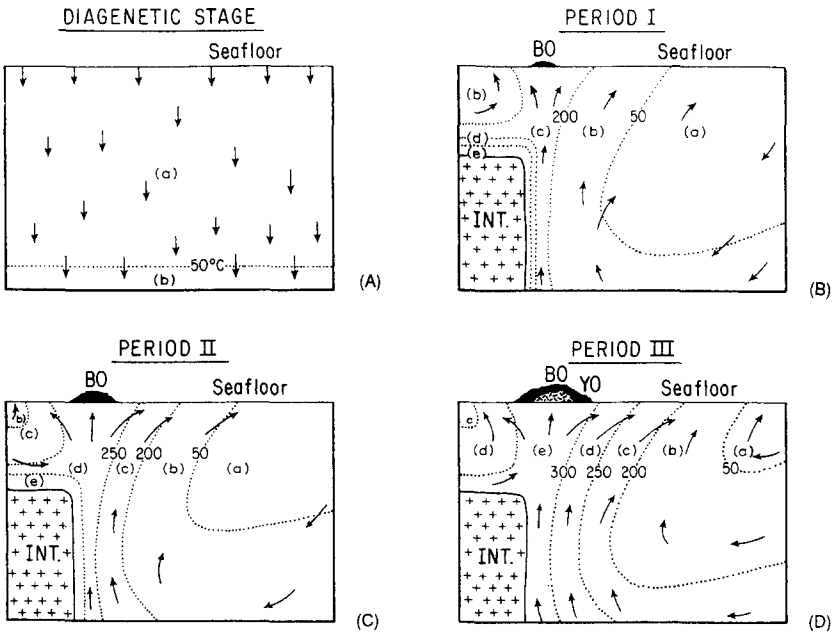

Fig. 11. A model for the evolution of alteration zoning around the Kuroko deposits. (A) diagenetic (zeolite-I stage), (B) early hydrothermal (zeolite-II and montmorillonite) stage, (C) intermediate (transitional) hydrothermal stage, (D) thermal maximum (sericite/chlorite) stage. *INT*: intrusive, *a*: zeolite-I assemblage, *b*: zeolite-II assemblage, *c*: montmorillonite stage, *d*: mixed layer clay assemblage, *e*: sericite/chlorite assemblage. From Pisutha-Arnond and Ohmoto (1983).

also be used to form calcite, resulting in the depletion of the CO_2 content of fluids, as seen in some of the DSDP pore fluids (Pisutha-Arnond and Ohmoto, 1983).

4.2.2. Zeolite-II stage

An intrusion of a heat source beneath the seafloor will cause local convection of the pore fluids, causing the wall rocks to be gradually heated (Fig. 11B). During the early and low-temperature stage of hydrothermal activity, hydration reaction (25) and cation exchange reaction (26) may continue. Organic matter in the marine sediments may begin to break down to produce CO_2 through reactions such as (3). An increase in the CO_2 content of the fluids may cause precipitation of calcite through reaction (4) and conversion of clinoptilolite and mordenite:

$$KNaAl_2Si_{10}O_{24} \cdot 8H_2O(\text{clinoptilolite}) + Ca^{2+} + CO_2(aq) \Rightarrow NaAlSi_2O_6 \cdot H_2O(\text{analcime}) + KAlSi_3O_8(\text{adularia}) + 5SiO_2(s) + CaCO_3(s) + 2H^+ + 6H_2O(l) \quad (28)$$

and:

$$CaAl_2Si_2O_{24} \cdot 7H_2O(\text{mordenite}) + 2Na^+ + CO_2(aq) \Rightarrow 2\,\text{analcime} + 6\,\text{quartz} + \text{calcite} + 2H^+ + 4H_2O(l) \quad (29)$$

These reactions cause the H_2O contents of rocks in zeolite-II zone to decrease from those in zeolite-I.

4.2.3. Montmorillonite stage

Increasing the temperature of the hydrothermal system to about 200°C may cause conversion of zeolites and Mg–Na-type smectites to Mg–Ca-type smectites (Fig. 12). The pH of the pore fluids may be buffered by smectite–carbonate equilibria at temperatures below ~250°C to values around 4.5 (Fig. 12). Under such low pH conditions, plagioclase is not stable, and is converted to Ca-rich smectite:

$$\text{plagioclase} + H^+ \Rightarrow Ca - \text{rich smectite} + \text{quartz} + Na^+ \quad (30)$$

4.2.4. Mixed-layer clay (transition) stage

At temperatures above ~250°C, Ca-rich and also Na-rich montmorillonite may become unstable and is replaced by expandable montmorillonite–illite mixed layer clays and sericite. Breakdown of plagioclase and formation of sericite (or sericite component in illite) by cation exchange reactions become important:

$$9\,\text{Na} - \text{montmorillonite} + 7K^+ \Rightarrow 7\,\text{sericite} + 12\,\text{quartz} + 4H^+ + 3Na^+ \quad (31)$$

and:

$$3NaAlSi_3O_8(s) + K^+ + 2H^+ \Rightarrow KAl_3Si_3O_{10}(OH)_2(s) + 6SiO_2(s) + 3Na^+ \quad (32)$$

These reactions cause an increase in the K content and a decrease in the Na content of the rocks.

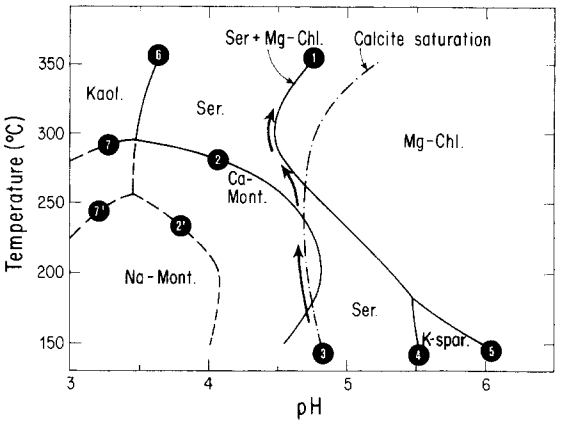

Fig. 12. Stability relationships among major alteration minerals around the Kuroko deposits (see Table 2 for the ΣNa, ΣK, ΣCa, ΣMg, ΣCl, ΣCO_2 values of the fluids). *1* = sericite + Mg-chlorite, *2* = Ca-montmorillonite + sericite, *3* = calcite saturation, *4* = sericite + K-feldspar, *5* = K-feldspar + Mg-chlorite, *6* = kaolinite + sericite, *7* = Ca-montmorillonite + kaolinite, *8* = Na-montmorillonite + kaolinite. The arrows indicate the estimated temperature–pH path for the Kuroko ore forming fluids during the thermal waxing stage. Modified from Pisutha-Arnond and Ohmoto (1983).

4.2.5. Sericite / chlorite stage

Reactions (31) and (32) continue to higher temperatures, which result in almost complete conversion of montmorillonite and plagioclase to sericite (see Fig. 11D). Calcite becomes unstable under the pH conditions where sericite is stable at temperatures above ~300°C (see Fig. 12). Mg–Ca-type smectite

is converted to Mg-rich chlorite. These processes cause further depletion in the Na and Ca contents and an increase in the K and Mg contents of rocks in the sericite/chlorite zone. The pH of the high temperature fluids are likely to remain at around 4.5 as long as both sericite and chlorite are stable (see Fig. 12).

The pH of many hydrothermal fluids along the mid-ocean ridges, however, has been calculated to be much lower, at ~ 3.5 (see Table 2). The lower pH is due to the lower K contents in basaltic rocks, which makes it difficult to form large quantities of sericite. In fact, one of the characteristics of VMSDs which occur in basaltic rocks is the absence of sericite in the central alteration zone (e.g., Franklin et al., 1981; Urabe et al., 1983). The pH of fluids in basaltic systems may be controlled by chlorite–kaolinite (pyrophylite) equilibria.

4.2.6. Kaolinite

Kaolinite occurs as patches, rather than as a well defined alteration zone, in montmorillonite and sericite–chlorite zones of some Kuroko deposits (e.g., Ijima, 1974; Utada et al., 1981). Kaolinite is especially abundant in the Nurukawa deposit in northern Honshu, Japan. The formation of kaolinite requires an acid (pH < ~ 3.5) solution (see Fig. 12). A possible mechanism to produce an acid in felsic volcanic environments, as suggested by Burnham and Ohmoto (1980), is the hydration of $SO_2(g)$ during cooling of a magmatic gas to temperatures below ~ 400°C by the following reaction:

$$4SO_2(g) + 4H_2O(1) \Rightarrow H_2S(aq) + 3H^+ + 3HSO_4^- \quad (33)$$

The presence of kaolinite, therefore, may suggest the

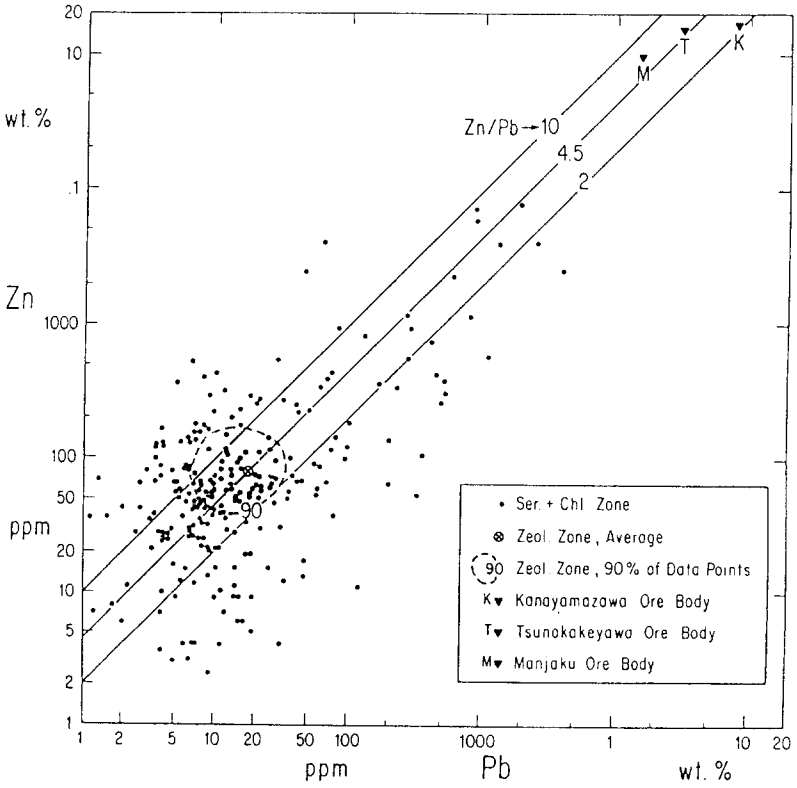

Fig. 13. Comparison of Pb and Zn contents of felsic volcanic rocks from different alteration zones in the Fukazawa area, Japan. Note that the Zn/Pb ratio of the largest Kuroko ore body in the area (Tsunokakezawa ore body) coincide with the average Zn/Pb ratio of the "unaltered" volcanics. From Ohmoto et al. (1983).

passage of magmatic volatiles during some stages of the development of alteration zones.

4.3. Leaching of ore metals from rocks

The heavy metal contents of volcanic rocks in the zeolite zone around the Kuroko deposits are essentially unchanged from those of "unaltered" volcanics (Fig. 13). However, about one-third of the rocks from the montmorillonite and sericite/chlorite zones are depleted in Zn, Pb and Cu, and the other two-thirds are either unchanged from the unaltered volcanic rocks or enriched in these metals; the magnitudes of both the enrichment and the depletion of these metals are increased from the montmorillonite zone to the sericite zone (Fig. 13). The enrichment of these ore metals in the wall rocks near the sites of ore deposits was expected, but the depletion was not. Many rocks in the sericite/chlorite zone have lost essentially all their Zn ($\sim$ 75 ppm), Pb ($\sim$ 10 ppm), and some Cu (a few ppm depletion from $\sim$ 70 ppm in the unaltered rocks).

The depletion of ore metals in the wall rocks is the best evidence that the hydrothermal fluids were undersaturated with respect to the metal-bearing mineral phases, and that the fluids were able to leach ore metals from the country rocks. This is an important evidence against the magmatic hydrothermal model for the heavy metals in the Kuroko ore-forming fluids. Most magmatic hydrothermal theories (e.g., Urabe, 1987) have postulated high concentrations of heavy metals in the fluids (e.g., $>$ 1000 ppm for each of Zn, Pb and Cu), but such fluids are supersaturated with respect to sphalerite, galena and chalcopyrite at $T = \sim 350$°C and pH = $\sim$ 4.5. Magmatic fluid, if they were important, would have precipitated most of the metals in the stockwork zone and below, and at temperatures above 400°C.

The concentration values for the heavy metals in the Kuroko fluids, estimated by Ohmoto et al. (1983), are remarkably similar to those measured for the MOR fluids: in units of mmol/kg H_2O, $\sim$ 0.1 for Fe, $\sim$ 0.01 for Cu, and $\sim$ 0.1 for Zn (see Table 2). The similarities suggest that the metal enrichment processes for the Kuroko hydrothermal fluids and the MOR fluids were basically the same.

Because Zn and Pb in the country rocks occur mostly in phases that become unstable during interaction with heated seawater, such as ferrous-bearing minerals for Zn and feldspar for Pb (Wedepohl, 1969), and because the solubilities of sphalerite and galena are high, the metal ratios in the fluids may become essentially identical to those in the footwall rocks. Indeed this appears to have been the case in the Kuroko hydrothermal systems. The Pb/Zn ratios of major ore bodies at the Fukazawa mine are essentially identical to those of the underlying volcanic rocks (see Fig. 13). The Zn/Cu ratios of the ores are, however, not the same as those in the country rocks, because the solubility characteristics of chalcopyrite are quite different from those of sphalerite and galena. The solubility of chalcopyrite depends on the redox state of fluids and is generally much less than those of sphalerite and galena.

Another type of data suggesting that the metals in the hydrothermal fluids were derived from leaching of country rocks is the Pb isotopic compositions of ores and country rocks (Fehn et al., 1983). In the Kosaka area of the Hokuroku district, the Pb isotopic compositions of the ores lie between those of the footwall volcanics and those of the underlying sedimentary rocks (Tertiary sandstones and pre-Tertiary phyllites), suggesting that the ore lead was a mixture of lead from various rock types in the footwall rock sequence (Fig. 14). In this area, the thickness of the footwall volcanic rocks is only about 200 m. In the Fukazawa area, where the footwall volcanics are at least 1 km in thickness, the ore lead also shows the isotopic characteristics of both the volcanics and the basement rocks.

An interesting feature noted by Fehn et al. (1983) is the existence of a clear difference in the Pb isotopic compositions between the yellow ores and the black ores (Fig. 14). The Pb in the yellow ores approaches the isotopic composition of the volcanic rocks; while the Pb in the black ores approaches that of the basement rocks. According to the model of ore growth shown in Fig. 4, the Pb in the yellow ores is probably a remnant of the earlier black ores, while the Pb in the black ores is a mixture of Pb transported by the hydrothermal fluids of all stages. Then, the observed relationship in the Pb isotopic composition of the yellow and the black ores suggests that the earlier fluids acquired Pb (and probably the other metals) largely from the stratigraphically shallower units (volcanics), while the later fluids acquired con-

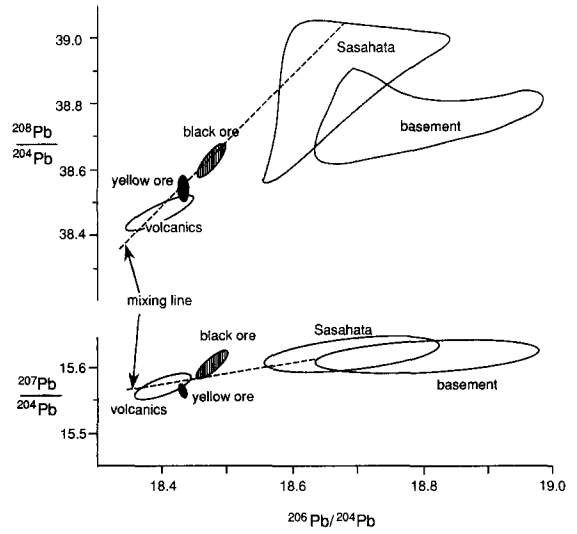

Fig. 14. Pb isotopic composition of rocks and ores in the Kosaka area, Japan. Note that the ore Pb lies on a mixing line between the Pb in the volcanic rocks and the Pb in the Sasahata Formation and the basement rocks. Rocks from the Sasahata Formation, a sandstone/conglomerate unit between the basement rock and the volcanics, has the Pb isotopic composition essentially identical to the basement rocks. Modified from Fehn et al. (1983).

siderable amounts of metals from the lower units (sedimentary rocks). This change with time in the dominant source rocks for the heavy metals in the ore-forming fluids may be a simple reflection of the fact that the metals in the volcanic rocks are easily leachable by low-temperature (earlier) fluids, but those in the phyllites are leachable only by higher-temperature (later) fluids. It may also reflect an expansion of the hydrothermal circulation system corresponding with the cooling of a heat source (Solomon, pers. commun., 1995).

4.4. Leaching of sulfur from rocks, and reduction of seawater sulfate by rocks

The $\delta^{34}S$ values of sulfides in VMSDs of Phanerozoic age are generally positive, with an average difference from the $\delta^{34}S$ value of contemporaneous seawater sulfate of about 15‰ (Sangster, 1968). This observation led Sangster (1968) to suggest that the sulfide–sulfur in VMSDs was generated locally by bacterial reduction of seawater sulfate. One of the serious problems with this model is the fact that the sulfur isotopic fractionation factors associated with bacterial sulfate reduction in marine environments, either within unconsolidated sediments or in the water columns of euxinic basin water, are typically 45 ± 20‰, rather than ~ 15‰ (Ohmoto et al., 1991). Fractionation factors around 15‰ have been found under some laboratory conditions (see review by Ohmoto, 1992), and possibly in Archean oceans (Ohmoto and Felder, 1987; Ohmoto, 1992), but are unlikely to have been common in Phanerozoic oceans.

There is abundant evidence suggesting that the high-temperature hydrothermal fluids transported re-

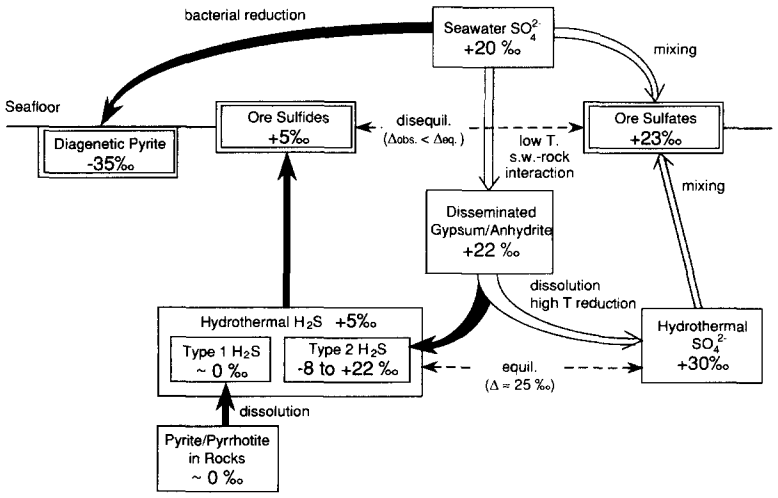

Fig. 15. Sulfur isotope systematics of the Kuroko system.

duced sulfur (H_2S) as well as metals. For example, in the alteration zones around the Kuroko deposits, the amounts of ferrous-bearing minerals (pyroxene, magnetite) and the magnetic susceptibility of rocks are decreased, but the pyrite contents are increased significantly, indicating sulfidization of rocks by hydrothermal fluids (Green et al., 1983). Thermodynamic calculations made by Ohmoto et al. (1983) suggest the H_2S contents of the Kuroko hydrothermal fluids were between 10^{-5} and 10^{-2} *m* (Table 2), which are similar to those found in the MOR hydrothermal fluids (Table 2).

Systematics of sulfur isotopes in the Kuroko system, as interpreted by Ohmoto et al. (1983) and Eldridge et al. (1983), are illustrated in Fig. 15. The $\delta^{34}S$ values of diagenetic pyrites in mudstones located at > 1 km away from the Kuroko deposits, but of the same stratigraphic horizons, range from −45 to −20‰ (average, −35‰), indicating that these pyrites were formed by bacterial reduction of seawater SO_4^{2-} with the kinetic isotopic fractionation factors of around −55‰. The $\delta^{34}S$ values of pyrite in mudstones gradually increase to the massive ore values (5 ± 3‰) with increasing grade of alteration, indicating hydrothermal imprints on biogenic pyrites. Accompanying this change in the $\delta^{34}S$ values, pyrite changes both its morphology, from a fine-grained framboidal form to a coarse-grained euhedral form, and its Ni/Co ratio (Eldridge, 1984).

The hydrothermal H_2S ($\delta^{34}S = 5 \pm 3$‰) appears to be the mixtures of two types of H_2S: type-1 H_2S, generated by leaching of sulfide minerals in the footwall rocks ($\delta^{34}S = 0 \pm 5$‰); type-2 H_2S, by non-bacterial reduction (i.e., reduction by Fe^{2+}-bearing minerals and/or by organic carbons) of seawater SO_4^{2-} (+20‰). In an earlier model proposed by Ohmoto and Rye (1974, 1979), seawater SO_4^{2-} was thought to be reduced directly to H_2S. However, it is more likely that seawater SO_4^{2-} was first fixed in the footwall rocks as fine-grained disseminated gypsum or anhydrite ($\delta^{34}S = \sim +22$‰) through reactions (26) and (27) during the downward percolation of the seawater at temperatures below ~ 150°C; this gypsum or anhydrite may be subsequently dissolved at higher temperatures, and partially reduced to H_2S. Such a scenario is supported by: (1) the ubiquitous occurrences of disseminated gypsum and anhydrite in the zeolite-facies rocks; (2) the rare occurrence of disseminated sulfates in the higher-grade alteration zones, especially in the sericite/chlorite zone; (3) the decreasing Fe^{2+}/Fe^{3+} ratios of volcanic rocks in the higher-grade alteration zone; and (4) a recognition that the estimated ΣSO_4^{2-} contents of the Kuroko ore-forming fluids, $\sim 10^{-3}$ *m*, agree with the values for fluids that are saturated with anhydrite at temperatures below ~ 300°C (Ohmoto et al., 1983).

Sulfate reduction by Fe^{2+}-bearing minerals occurs readily at temperatures above ~ 200°C where the isotopic equilibrium is also attained between SO_4^{2-} and H_2S if the two species coexisted for a period of more than ~ 10 days (Ohmoto and Lasaga, 1982). The $\delta^{34}S$ value for type-2 H_2S depends on the degree of sulfate reduction, temperature, and the $\delta^{34}S$ value of gypsum and anhydrite. The equilibrium fractionation factor between SO_4^{2-} and H_2S is ~ 30‰ at 200°C, ~ 25‰ at 250°C, and ~ 20‰ at 350°C (Ohmoto and Lasaga, 1982). Therefore, the $\delta^{34}S$ value for type-2 H_2S, generated from anhydrite of +22‰, may range from about −8‰ when the degree of reduction was small (e.g., $m_{H2S}/m_{\Sigma SO4} < 0.1$) and $T \approx 200$°C to about +22‰ when the sulfate was completely reduced (see Fig. 15).

The hydrothermal SO_4^{2-} that was in equilibrium with H_2S of +5‰ should have $\delta^{34}S$ values around +30‰ at 250°C. Mixing of such SO_4^{2-}-bearing fluids with local seawater formed anhydrite and barite with $\delta^{34}S$ values around +23‰. The sulfur isotopic relationships between sulfides and sulfates in the ores are typically disequilibrium ones; the observed fractionation factors are less than the equilibrium ones (see Fig. 15).

Sulfur isotopic systematics of other submarine hydrothermal systems are basically the same as those for the Kuroko systems, especially with respect to the presence of two types of H_2S (one produced by leaching of country-rock sulfides and the other by reduction of seawater sulfate) in the hydrothermal fluids, the presence of two types of SO_4^{2-} in the ore sulfates (hydrothermal and local seawater), and the disequilibrium isotopic relationships between ore sulfides and sulfates. The examples include the modern submarine hydrothermal systems on the East Pacific Rise (Styrt et al., 1981; Bluth and Ohmoto, 1986), on the Juan de Fuca Ridge (Goodfellow and Franklin, 1993), and in the Red Sea (Shanks and

Bischoff, 1980; Zierenberg and Shanks, 1988), and also many ancient VMSD (Ohmoto, 1986a, Ohmoto, 1992).

Variations in the sulfur isotopic characteristics of submarine hydrothermal systems reflect the variations in: (1) the degree of sulfate reduction during generation of type-2 H_2S (i.e., the $\Sigma SO_4^{2-}/H_2S$ ratio of fluids), which depends largely on the temperature and lithology (i.e., the abundance of reductants) of hydrothermal systems; (2) the mixing ratio of type-1 and -2 H_2S; and/or (3) the $\delta^{34}S$ values of seawater SO_4^{2-}. In general, the fluids which attained higher temperatures and those developed in mafic rocks, such as in the mid-oceanic ridges, tend to attain higher proportions of country rock sulfides and lower $\Sigma SO_4^{2-}/H_2S$ ratios (i.e., more reduced); sulfate minerals in such systems have $\delta^{34}S$ values essentially identical to the seawater value. In contrast, the hydrothermal systems developed in dominantly felsic rocks, where the Fe^{2+}-contents are lower, tend to produce sulfate minerals with higher $\delta^{34}S$ values.

The $\delta^{34}S$ value of seawater SO_4^{2-} varied between +10 and +30‰ during the Proterozoic and Phanerozoic eras, but were probably around +2‰ during the Archean (Ohmoto, 1992; Ohmoto et al., 1993). The sulfur isotopic systematics of the ~2.7 b.y. old Hemlo deposits (Fig. 16) and of other Archean VMSDs (Fig. 17) are also basically the same as those of the Kuroko systems: the sulfide minerals appear to have formed from hydrothermal fluids that contained the two types of H_2S, and the sulfate minerals by mixing of SO_4^{2-}-bearing hydrothermal fluids with SO_4^{2-}-rich seawater.

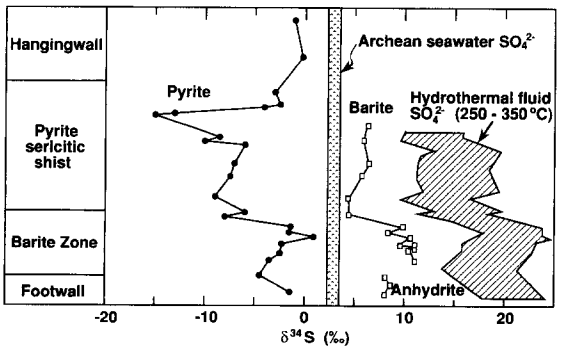

Fig. 16. Sulfur isotope systematics of the ~2.7 b.y. old Hemlo deposit, Canada. The $\delta^{34}S$ values of sulfide and sulfate minerals are from Cammeron and Hattori (1985). The $\delta^{34}S$ values for the hydrothermal SO_4^{2-} are estimated from the $\delta^{34}S$ values of pyrites and the equilibrium fractionation factors between pyrite and SO_4^{2-} of Ohmoto and Lasaga (1982). The $\delta_{34}S$ value of Archean seawater SO_4^{2-} is from Ohmoto (1992).

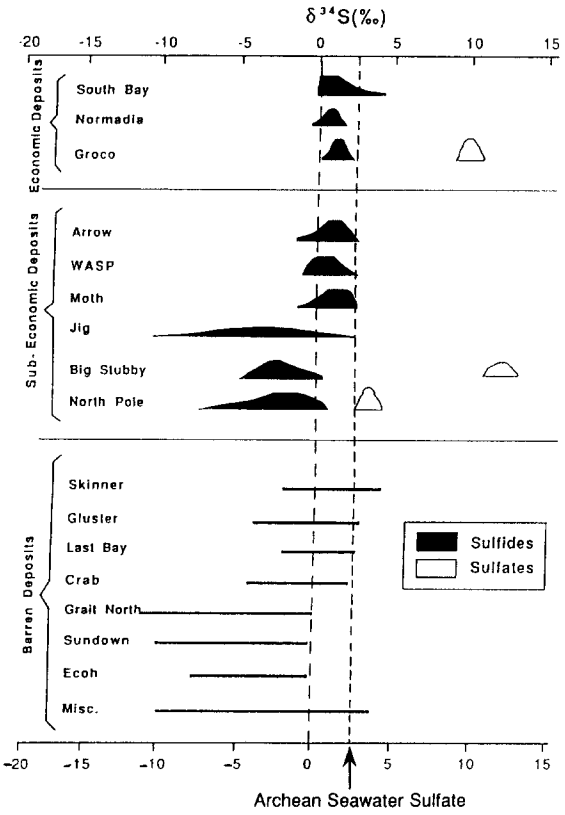

Fig. 17. Comparison of the $\delta^{34}S$ characteristics and the economic importance (i.e., size) of Archean VMSDs. Modified from Ohmoto (1992).

Seccombe (1977) recognized a correlation between the size of Archean VMSDs and the $\delta^{34}S$ values of sulfides: the $\delta^{34}S$ values of larger (i.e., economic size) VMSDs generally fall between 0‰ and about +2‰, while those of smaller (barren) VMSDs tend to be more variable and negative (see Fig. 17). Such a correlation can also be explained by the model presented in Fig. 15. When the submarine hydrothermal processes operate vigorously (i.e., higher temperature and larger scale plumbing system), the hydrothermal fluids will attain a larger quantity of type-1 H_2S ($\delta^{34}S \approx 0$‰) because of increasing solubility of sulfides at higher tempera-

tures; a larger quantity of type-2 H_2S with $\delta^{34}S$ value similar to the $\delta^{34}S$ of seawater will also be produced. A consequence of such processes will be the $\delta^{34}S$ of ΣH_2S fall between 0 and the $\delta^{34}S$ of seawater ($\sim +2‰$ during Archean), with relatively little variation. In contrast, when the submarine hydrothermal processes operate less intensively, acquisition of type-2 H_2S, which tends to have much lower $\delta^{34}S$ values than the $\delta^{34}S$ of seawater, may cause the $\delta^{34}S$ values of smaller VMSDs to become more variable, with a tendency toward negative values.

The above comparisons of the sulfur isotopic systematics between the Archean and the younger VMSDs suggest that the processes of submarine hydrothermal mineralization and the concentration of seawater sulfate have been basically the same throughout geologic time.

4.5. Hydrology of the plumbing system

4.5.1. Geometry

A schematic diagram illustrating the geometry of a plumbing system of a typical Kuroko ore cluster is shown in Fig. 18, and a summary of the hydrological characteristics in Table 3. (Note that Fig. 18 is intended to illustrate only the relative sizes of the rock, fluid, and heat source, and not the realistic fluid flows.) Generally, the discharge area of hydrothermal fluids, as demonstrated by the $\delta^{18}O$ and $\delta^{34}S$ haloes, is about 1.5×3 km: the extent of the montmorillonite zone is about one half of the area. Within this area, ~ 3 to ~ 20 ore bodies with an average size of ~ 1 million tons of ore occur as an ore cluster. Within a mining district, several ore clusters occur.

Ore bodies in the same ore cluster appear to have formed essentially contemporaneously, but those of different ore clusters may not. For example, in the Hokuroku district, seven ore clusters, which differ in age by more than a few million years and are separated by an average distance of ~ 8 km from each other, have been recognized (see Fig. 21). (The spatial regularity in the occurrences of VMSDs in mining districts was first suggested by Solomon in 1976). Distinct differences exist in the trace element and Pb isotopic characteristics among ores belonging to different ore clusters (Ohmoto and Takahashi, 1983; Fehn et al., 1983; Lenagh, 1985). Such features suggest that the hydrothermal system responsible for one ore cluster was not related to that of the others; thus, the lateral dimension of a plumbing system was less than ~ 8 km. The *minimum* depth of fluid circulation was 1 km, because the Pb isotopic characteristics of the basement rocks have been recognized in the ore deposits which are underlain by more than 1 km thick volcanic rocks (see earlier section of "Leaching of ore metals from rocks").

Table 3
Summary of hydrological characteristics of an average Kuroko system

Fluid discharge zone	4.5 km^2 (= 1.5×3km)
Amount of ore (total)	3–50 mil. tons
Zn, Ba	1 mil. tons each
Mass of fluid	10^{11} tons (= 100 km^3 of seawater)
Mass of rocks interacted	10^{11} tons (= 40 km^3 = $3 \times 5 \times 2.5$ km)
Heat source (size)	10 km^3 (= $1.5 \times 3 \times 2$ km)
Duration	200–10000 years
Fluid mass flux	10^6 g/cm^2/year in fluid conduits

An aquifer (or aquifers) may have existed at some depths. If an intrusion of a heat source occurs near the aquifer(s), it may cause to boil water in the aquifer(s) (Cathles, 1993). Such a process may have been the main reason for the salinity variation in some Kuroko ore-forming fluids and also in some MOR hydrothermal fluids (see Table 2).

The total amount of sulfide ore in an ore cluster varies from ~ 3 to ~ 50 million tons, but the amount of Zn (and also of Ba) in an ore cluster is fairly constant at about 1 million tons (Ohmoto et al., 1983). If only 10 ppm of Zn is leached from rocks containing 70 ppm of Zn (see section of "Leaching of ore metals from rocks"), the mass of rock required to supply 1 million tons of Zn is $\sim 10^{11}$ tons (i.e., ~ 40 km^3 in volume or $\sim 3 \times 5 \times 2.5$ km in size). This mass of rock, with only the 1 wt% Fe^{2+} content, has a capacity to reduce ~ 70 million metric tons of seawater sulfate sulfur to sulfide sulfur, which is more than ~ 10 times the amount of reduced sulfur in an ore cluster. If only ~ 10 percent of the metals leached from the rocks was fixed in ore deposits due to the inefficiency in the depositional mechanisms, then the required mass of rocks becomes $\sim 10^{12}$ tons, corresponding to a rock volume of ~ 400 km^3, or $\sim 8 \times 8 \times 5$ km.

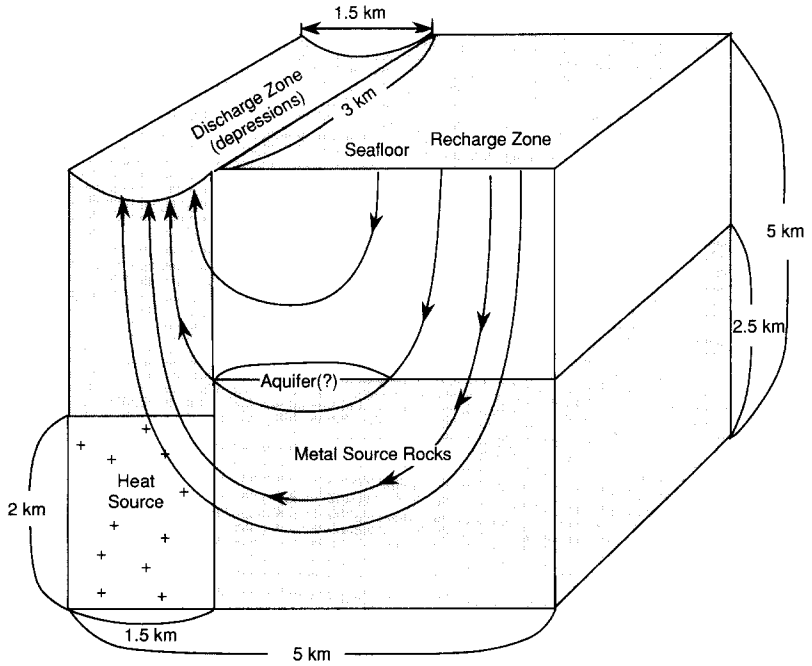

Fig. 18. Schematic representation of the hydrology of the average Kuroko-forming system.

From a similar calculation, Solomon et al. (1987) have suggested that a rock volume of 400 km^3 ($10 \times 10 \times 4$ km) was needed to form the Rosebery deposit with 4 million tons of zinc, if 10 ppm of Zn was leached from a third of the convective cell.

4.5.2. Mass of fluids

Since the average Zn content of the Kuroko ore fluid was ~ 10 ppm, the mass of fluid required to precipitate ~ 1 million tons of Zn would become $\sim 10^{11}$ tons if all the metals in the fluid precipitated during the interaction with cold seawater, $\sim 10^{12}$ tons of fluid is required with 10 percent efficiency in precipitation. The water/rock mass ratio of the system, integrated over the life of hydrothermal activity, is, therefore, ~ 1 to ~ 10.

The integrated water/rock ratios for rocks in the fluid-discharge zones are much higher than the water/rock ratio for the entire system, because the discharge area is much smaller than the total system. Based on the mass balance between rocks and seawater of Mg, Ca and the oxygen isotopes, the minimum integrated water/rock mass ratios have been estimated to be ~ 2 for the montmorillonite zone and ~ 20 for the sericite/chlorite zone. (Ohmoto et al., 1983).

4.5.3. Heat source

An equation for heat balance between fluids and heat source (intrusive), according to Cathles (1983), is as follows:

$$Q/M = (C_r/C_f)\ln(\Delta T_o/\Delta T_t) \quad (34)$$

where Q is the mass of water required to cool an intrusion with mass M, ΔT_o and ΔT_t are the temperature contrast between the intrusion and the country rocks at the time of intrusion and after some time, respectively; C_r and C_f are the heat capacities of water-saturated rock formation, and the fluid, respectively. From this equation, the mass of intrusion required to heat $\sim 10^{11}$ tons of seawater to an average of 200°C is $\sim 3 \times 10^{10}$ tons, equivalent to ~ 10 km^3 in volume, or $\sim 1.5 \times 3 \times 2$ km in size, if the initial temperature of the intrusive was 800°C and that of the country rock was 100°C.

From the analyses of the distance between ore deposits, Solomon et al. (1987) have suggested that the heaters for the Kuroko deposits were plutons of

high aspect ratio, but those for some Canadian and Tasmanian VMSDs the heaters were sills.

4.5.4. Duration of hydrothermal activity

The $\delta^{34}S$ values of diagenetic pyrite in marine shales have been found to be related to the sedimentation rate of the clastic sediments (Ohmoto and Goldhaber, 1996). Using the empirical curve relating the $\delta^{34}S_{pyrite}$ values to the sedimentation rate leads to sedimentation rates of ~0.01 to ~0.6 cm per year for mudstones with the $\delta^{34}S$ values of −40 to −20‰, i.e., typical values for the mudstones associated with the Kuroko deposits and the Red Sea deposits.

The total thickness of interbedded mudstones in a massive sulfide body of a typical Kuroko deposit is ~1 m. The above sedimentation rates implies a time of ~200 to ~10000 years to form an ore body. These values are in good agreement with those estimated by Cathles (1983) from two dimensional numerical modeling of fluid flow associated with a pluton, 2.3 km wide and 3.3 km high, emplaced 1.7 km below the seafloor (see Fig. 19). The duration of ~100 to ~1000 years for a single cycle of hydrothermal activity has also been suggested for the hydrothermal activity at sites along the East Pacific Rise (e.g., Rona and Scott, 1993) and the Red Sea hydrothermal systems (Fig. 20), and may be typical of submarine hydrothermal systems.

The kerogens in mudstones in the sericite/chlorite zone are not thermally matured, and show essentially the same characteristics as those in the zeolite zone (Kumita et al., 1983; Gize and Ohmoto, unpublished data). An application of an empirical curve for kerogen types versus time, which was established in petroleum-bearing sedimentary basins, to the organic matter in the Hokuroku district gives temperature values of only ~100°C even in the sericite/chlorite zone (Kumita et al., 1983; Gize and Ohmoto, unpublished data). The apparent contradiction of the kerogen temperatures to the temperatures obtained by fluid inclusions and silicate mineral assemblages can be explained by the short-lived nature of the high temperature hydrothermal activity.

Although a single cycle of hydrothermal activity appears to have lasted for <10000 years, intermittent hydrothermal activity, caused by intrusions of new heat sources, appears to have continued in most

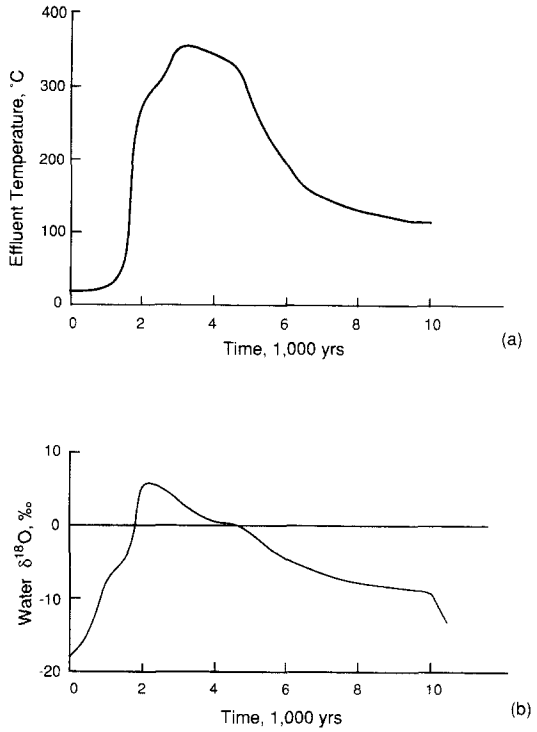

Fig. 19. Numerical modeling of thermal and isotopic history of a submarine hydrothermal system associated with a magma of 1.0 km wide and 3.25 km high; the top of the magma is 1.5 km below the seafloor. (a): temperature of discharging fluid, (b): $\delta^{18}O$ of discharging fluid. Modified from Cathles (1983).

VMSD districts, evidenced by the high-temperature alteration of the hanging wall rocks which commonly extends several hundred meters above the

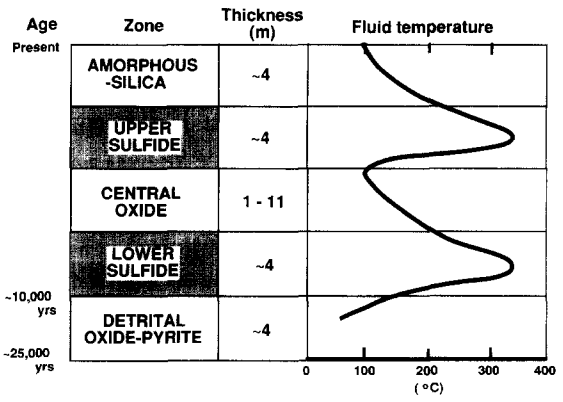

Fig. 20. Thermal and mineralization history of the hydrothermal system in the Atlantis II Deep, Red Sea. Constructed from the data in Pottorf and Barnes (1983).

main ore zone, and the common occurrence of several stacked ore bodies and/or later vein mineralization (Green et al., 1983). For example, in the Matsumine area of the Hokuroku district, three major hydrothermal events formed three stacked ore bodies within a period of ~ 1 m.y. (Tanimura et al., 1983). In the Red Sea, two major episodes of sulfide mineralization have been recorded during the past 10 000 year period (Fig. 20). The $^{40}A/^{39}A$ age determination on fuchsite in the alteration zone of the Kidd Creek deposits suggests that hydrothermal activity continued (intermittently?) approximately 100 million years after the sulfide mineralization ~ 2700 m.y. ago (Smith et al., 1993).

In each VMSD area, the most important mineralization appears to have taken place during the first cycle of hydrothermal activity. Where stacked ore bodies occur, the lowest ore bodies are generally larger. Such characteristics are accounted by the seawater–rock interaction model for the origin of ore-forming fluids responsible for VMSDs because readily soluble metals and reduced sulfur in the country rocks are depleted by the first cycle of hydrothermal activity, and the capacity for rocks to reduce seawater sulfate (i.e., the ferrous content) diminishes with the extent of reaction through time.

4.5.5. Fluid flow rates

Cathles (1983) has suggested that the fluid flux was > 2900 g/cm^2/year in the stockwork ore zone of the Kosaka mine in the Hokuroku district, because the thermal gradient in the plumbing system, as indicated from the fluid inclusion homogenization temperatures, was less than 30°C/km.

Another method for estimating the fluid flux is from the hydrodynamic characteristics summarized in Table 3. If ~ 10^{11} tons of fluids discharged in a ~ 5 km^2 area in ~ 1000 years, the average fluid flux would be ~ 2000 g/cm^2/year. Because the fluid was not uniformly discharged within this area, but was channeled by several fracture zones, the actual fluid flow rates in the fracture zone must have been several orders of magnitudes higher than the above values. For example, if all the fluids were channeled through 100 pipes with an average diameter of 10 m, the fluid flux would become ~ 1.3×10^6 g/cm^2/year or ~ 3500 g/cm^2/day. This flux value may be translated to mean that the discharging fluid traveled in the pipes at an average rate of ~ 35 m/day, or that it took ~ 30 days to travel from the depth of 1 km to the seafloor. Interestingly, this flow rate is comparable to the values suggested by Baker and Lupton (1990) for the fluid responsible for a huge thermal cloud discovered on the Juan de Fuca Ridge in 1986; they have suggested from a heat balance calculation that the 350°C water must have vented from a depth of 200 to 2000 m in 2 to 20 days.

5. Controls of spatial and temporal distribution of volcanogenic massive sulfides

Major questions on the genesis of VMSDs are causes for the regularities in their spatial and temporal distribution that have been observed in many mining districts. For example, the major VMSDs in the Iberian pyrite belt are distributed regularly at a distance of about 20 km (Solomon, 1976; Solomon, pers. commun., 1995). A spacing of ~ 5 to ~ 10 km has been recognized for the ore clusters in the Hokuroku district (Scott, 1978; Ohmoto and Takahashi, 1983). The VMSDs of a mining district typically occur within a narrow stratigraphic interval. For example, their formation in the Hokuroku district were restricted to a period between 17 and 11 m.y. ago, in spite of the fact that submarine volcanism occurred over a much longer period of time, from ~ 25 m.y. to ~ 5 m.y. ago (Ohmoto and Takahashi, 1983). In other words, the formation of VMSDs was related to only certain types and/or periods of submarine volcanism.

5.1. Submarine calderas and Kuroko ore genesis

The formation of Kuroko deposits took place shortly after a major episode of volcanic activity which produced thick accumulations of tuffs and tuff breccia (Horikoshi, 1969; Ishihara, 1974). This temporal relationship was important in the development of a theory by Ohmoto (1978) that the formation of submarine calderas played a key role in the genesis of VMSDs, much like the role played by subaerial calderas where creation of large fracture systems and providing a local heat source for convection of meteoric water was involved in the formation of many

vein deposits, such as those in the San Juan district, Colorado (Casadevall and Ohmoto, 1977).

There are apparently several centers of felsic igneous activity in the Hokuroku district (Fig. 21), as shown by the relative ages, compositions and spatial distribution of associated igneous and sedimentary rocks (Ohmoto and Takahashi, 1983; Guber and Green, 1983). The centers are 5 to 10 km apart, and aligned subparallel to the basement fracture systems that were suggested by Scott (1978). Each volcanic center apparently was active at different times, at ~ 17 m.y. ago in the western part, at ~ 13 m.y. ago in the central part, and at ~ 11 m.y. ago in the eastern part. However, each had a similar history of initial fissure eruption of dacite and rhyolite lavas (Phase I), eruption of volcanic tuffs and tuff breccia, accompanying caldera subsidence (Phase II), Kuroko ore mineralization in the caldera depressions (Phase III), and, finally, resurgent cauldron activity (Phase IV).

A close temporal association of the formation of VMSDs with submarine calderas has been suggested in other mining districts, such as in the Bathurst district, Canada (Harley, 1979) and in the Mattabi district, Canada (Morton et al., 1991).

5.1.1. Roles of submarine depressions

A well-known cross-section of a Kuroko deposit by Sato (1973), which shows the massive sulfide body sitting on top of a rhyolite dome, has given many readers a serious misconception that the sulfide mineralization occurred on submarine highs. However, after a detailed structural analysis of the Kosaka deposits, Hashiguchi (1983) suggested that the ores accumulated in submarine depressions, and that the extrusion of dome-forming rhyolite occurred during and after mineralization. The doming was a major cause of the deformation and clastic textures of the ores but not of initial ore deposition.

In the Hokuroku district, the ore clusters occur in areas where tuffs and mudstones of the local stratigraphic section are much thicker than in the surrounding areas (Ohmoto and Takahashi, 1983), suggesting also that mineralization occurred in submarine depressions (Fig. 21). The Red Sea mineralization is confined in submarine depressions in the central rift zone; the hydrothermal activities on the mid-ocean ridges, such as Juan de Fuca Ridges, are

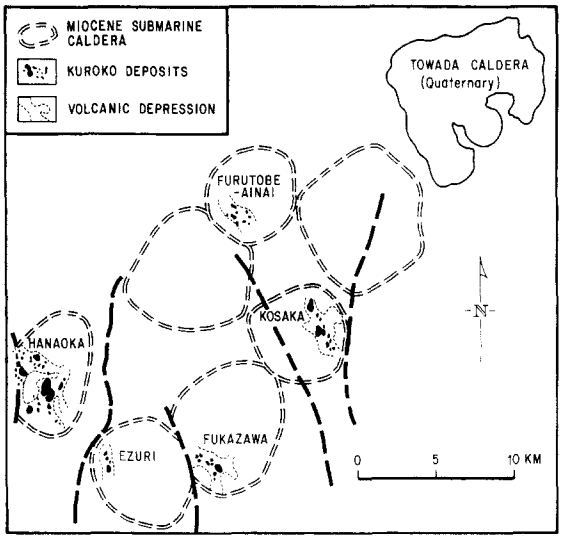

Fig. 21. Approximate locations of the Miocene submarine calderas in the Hokuroku district. Note that the calderas are aligned in the directions (NE–SW and NW–SE) of the dominant basement fractures. The Kuroko deposits are restricted to the depressions created by caldera formation. Modified from Ohmoto and Takahashi (1983).

observed in the central valleys of the rift zones (e.g., Goodfellow and Franklin, 1993). In the Kidd Creek deposits, thick organic-rich shales are confined in areas where massive sulfide bodies occur (Fig. 22), suggesting that the sulfide mineralization occurred also in submarine depressions.

Submarine depressions, particularly caldera depressions, are the most favorable areas for *formation* and *preservation* of massive sulfide ores for hydrological, physical and chemical reasons. For hydrological reasons, submarine depressions become the locus of discharging hydrothermal fluids. Lasaga (quoted in Ohmoto and Takahashi, 1983) has computed that the flow lines of discharging fluids, initially uniform at the depths below ~ 1 km from the seafloor, tend to converge toward the submarine topographic lows and that the fluid fluxes into the depressions are about three times greater than those into sea-floor highs if with similar permeabilities (Fig. 23). If the depressions were created by caldera subsidence, the rocks under the depressions would have a higher permeability than those under sea-floor highs because they would be more intensely fractured. This high permeability zone also would tend

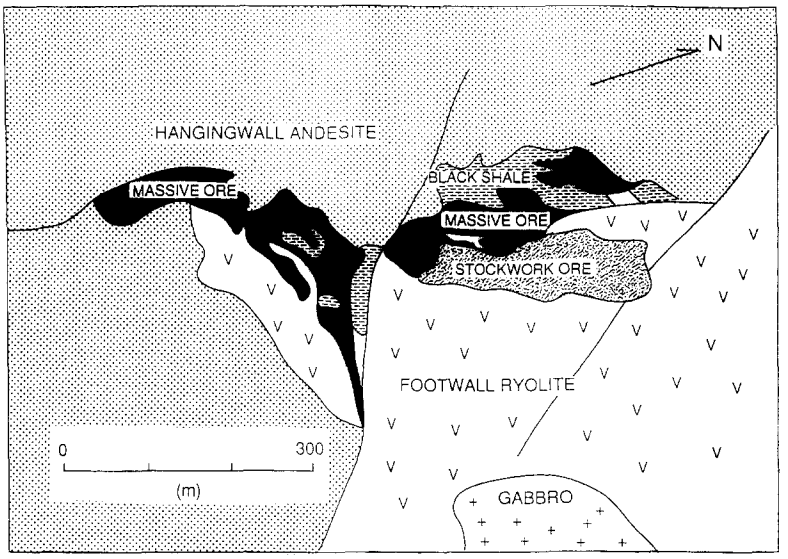

Fig. 22. A simplified geologic map of the Kidd Creek deposit (modified from Walker et al., 1975). Because the beds dip near vertically, the map can be viewed as a cross-section. The occurrences of thick organic-rich shales in areas of sulfide ore bodies suggest the ore-formation in submarine depressions.

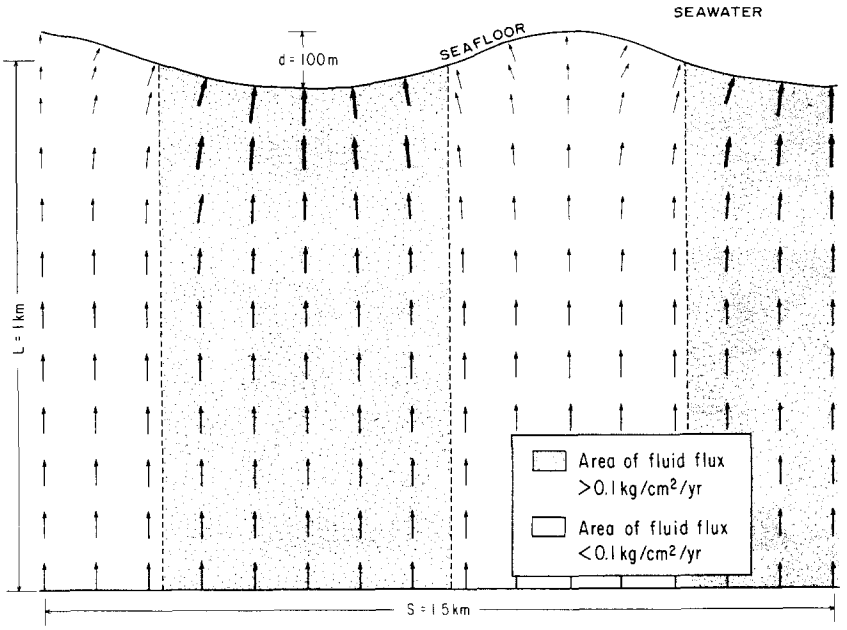

Fig. 23. Effects of seafloor topography on flow direction and fluxes of fluids discharging onto seafloor (computed by A.C. Lasaga and reproduced in Ohmoto and Takahashi, 1983). The boundary conditions set for the computations are: depressions 500 m wide and 100 m high; uniform fluid flux at a level of 1 km below the seafloor at 100 g/cm^2/year, uniform permeability of 1 mD for the rock system; a uniform density of 1 g/cm^3 and a uniform viscosity of 0.01 poise for the fluid.

to be hotter and have higher geothermal gradients than surrounding zones because it is a locus of magma intrusion. The combined effects of increasing permeability, temperature, and thermal gradient accentuate the tendency of discharging fluids to converge into the depressions.

Submarine depressions also act as traps for the ores; without a physical barrier, sulfide ores may be washed away by bottom currents. Graham et al. (1988) has found that the sulfide/sulfate chimneys on the East Pacific Rise are continuously being dissolved in local seawater. Preservation of sulfides and sulfates are facilitated in depressions because depressions are the preferential sites for accumulation of post-ore volcanoclastic sediments, which may shield the massive sulfides from oxidizing seawater. Hydrothermal H_2S may also accumulate in the water column within the depressions, possibly preventing ore disintegration by seawater.

The above discussion leads to a suggestion that an identification of submarine depressions where tuffs, tuff breccia, and mudstones are thicker than other areas is an important step toward a successful discovery of VMSDs.

5.2. Seawater depth

In order to form massive sulfide deposits on the seafloor, hydrothermal fluids must transport sufficient amounts of metals and reduced sulfur, each at concentration levels $> \sim 1$ ppm (or $> \sim 10^{-4}$ *m*). For fluids with the salinity of normal seawater, ~ 0.7 *m* ΣCl, to transport these amounts of Cu and other metals, the fluids must be heated to temperatures $> \sim 300$°C (Ohmoto et al., 1983). At pressures lower than ~ 200 bars, the fluids with $T \geq 300$°C boil; the vapor can not transport sufficient quantities of metals. Therefore, a hydrostatic condition required for the formation of Cu-rich massive sulfide deposits is seawater depths greater than ~ 2000 m. Note also that Cu-rich sulfide chimneys on the East Pacific Rise are forming from fluids with the salinities similar to normal seawater and temperatures around

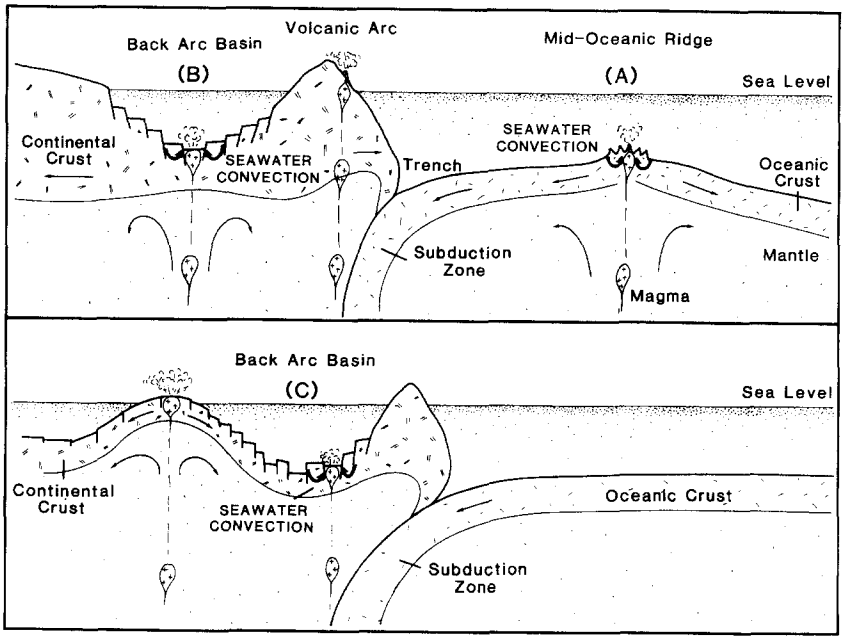

Fig. 24. Principal plate tectonic settings for deep-sea volcanism, submarine hot springs, and volcanogenic massive sulfide deposits. (A): mid oceanic ridges, (B): central part of continental rifts developed in thick crust (> 25 km), (C): flanks of back-arc spreading center developed in thin (> 25 km) crust.

350°C at the depths around 2600 m (e.g., Goldfarb et al., 1983).

The Hokuroku district was under shallow (< 200 m) seas until about 17 m.y. ago when the district subsided very rapidly to depths near 3500 m by a large scale tectonic activity (Guber and Merrill, 1983). This was probably an important reason why the Kuroko mineralization did not occur before about 17 m.y. ago.

Because the solubilities of heavy metals increase with increasing salinity, the concentration of Cu as well as that of Zn and Pb can be > 1 ppm in lower temperature solutions if the salinity was higher than that of normal seawater (e.g., ~ 200°C with ~ 20 wt% NaCl). The boiling temperature of fluid decreases with decreasing temperature and increasing salinity. Therefore, Cu-rich VMSDs can be formed in seas shallower than ~ 2000 m if the fluids were brine.

5.3. Tectonic setting

A few plate-tectonic settings favor the creation and persistence of deep submarine environments with active volcanism: mid-oceanic ridges, mid-continental rifts (e.g., the Red Sea), back-arc rifts, and the flanks of back-arc spreading centers (Fig. 24). Whether the Kuroko-bearing districts formed at the center of a back-arc rift (Cathles, 1983) or on the flanks of a back-arc spreading-center (Ohmoto, 1983) during the period about 15 m.y. ago remains a matter of discussion. Either model, however, proposes an extensional tectonic regime. This view is in contrast to the previously dominant view (e.g., Hutchinson, 1973) that the plate tectonic setting of Japanese islands during Miocene time was the same as today and the Kuroko mineralization occurred while under lateral compressional stress.

6. Controls of ore deposit types

The models presented above for the processes of ore growth and the processes of evolution of ore-forming fluids suggest that the chemical and mineralogical characteristics and the maturity (or size) of a VMSD is controlled largely by the following three parameters: (1) chemical and mineralogical compositions of the footwall rock sequence; (2) thermal structure of the seawater–rock system; and (3) composition of seawater which is influenced by paleogeography. These are summarized below:

6.1. Composition of footwall rocks

The geometry of an average Kuroko-forming hydrothermal system (Fig. 18) suggests that the chemical compositions of the hydrothermal fluids must be influenced by the mineralogical and chemical characteristics of the footwall rocks that occur in a ~ 5 × 5 km area around the deposits and the depth to ~ 5 km from the seafloor. Some of the important parameters of those rocks are: (1) the concentrations of readily extractable elements, including those from feldspars (Pb and Ba sources), Fe-bearing silicates (Zn, Cu and Fe sources) and volcanic glass (all metals); (2) the abundance of sulfide minerals (e.g., pyrite, pyrrhotite); (3) the concentrations of ferrous components and organic carbon, which determine the reducing capacity of rocks; and (4) the presence or absence of evaporites.

There are several associations of rock compositions with ore types. The main reason for the lower concentrations of Pb and Ba in VMSDs associated with basaltic rocks compared to those associated with felsic rocks (see Table 1) is that these elements are less abundant in mafic rocks. Higher concentrations of Fe^{2+} in basaltic rocks, compared to felsic rocks, would make hydrothermal fluids Cu-rich and more reduced than those associated with felsic rocks, and could promote the formation of chalcopyrite and pyrrhotite in the ores. Zn concentrations are, however, not strongly dependent on rock types.

Fluids heated to high temperatures would carry higher concentrations of H_2S and Fe if the footwall rock sequence contains more organic carbon and pyrite than normal felsic volcanic rocks (Ohmoto and Goldhaber, 1996). This enrichment of Fe and H_2S may explain why the VMSDs in the Iberian pyrite belt, where thick Devonian shales underlie a few-hundred meter thick volcanic sequence, contains so much more pyrite than typical VMSDs, but the Zn contents of these deposits are similar.

6.2. Thermal regime

6.2.1. Ore-type distribution within an ore cluster

The relationships among the maturity, ore type and size of VMSDs (Fig. 4) suggest that a regular spatial distribution of ore types would develop in an ore cluster. The deposits formed closer to the heat source would be the hotter, more matured type with larger pyrite cores and higher Cu/Zn and Cu/Pb ratios, while those developed further away would be smaller in size and of the black-ore type. Those formed furthest away from the heat source would be only hematite–quartz ores. Indeed, such regularities can be seen in several areas of the Hokuroku district (Ohmoto et al., 1983).

6.2.2. Ore deposit size versus igneous types

Although felsic intrusives may have lower initial temperatures than mafic intrusives, they tend to become much larger in size than the mafic intrusives (e.g., stocks versus dikes and sills) because of the difference in viscosity. Therefore, felsic intrusives tend to represent larger heat sources than mafic intrusives. This may be an important reason why all of the large VMSDs are associated with felsic rather than basaltic volcanism.

6.3. Composition of seawater and paleogeography

Seawater increases its salinity through evaporation, and also by dissolution of evaporites if they occur in the plumbing system; both processes are more likely to occur near the equatorial regions, such as in the Red Sea. Chloride-enriched seawater can transport higher concentration of metals compared to normal seawater if they were reacted with rocks at the same temperature; brine can continue to transport high concentrations of metals during the waning stage of submarine hydrothermal activity. Therefore, submarine hydrothermal systems developed in the equatorial regions tend to form bigger VMSDs than those developed in other regions.

With increasing salinity, the density of the fluid increases and the buoyancy decreases. When such dense fluids are discharged onto the seafloor, they may not mix with the overlying seawater as readily as lighter fluids, and may even form brine pools on the seafloor, much like those of the Red Sea. The sulfide ores formed from such brines may, therefore, be more widespread in geometry and poorer in anhydrite compared to VMSDs formed from ore fluids with salinities of normal seawater.

The concentration of sulfate in the local seawater may play an important role in the development of massive pyrite ores. If local seawater were sulfate-poor, anhydrite bodies may not develop on or beneath the seafloor during the reaction with hydrothermal fluids, and the paucity of anhydrite may eliminate one mechanism of pyrite formation (see section of "Fe-bearing minerals"). The oxygen content of local seawater may also affect the amount of polysulfide formed in the mixed fluid and could affect the amount of pyrite in ores (see "Fe-bearing minerals"). The oxygen content of seawater also influence the preservation of sulfide ores.

6.4. Evolution of VMSDs through geologic time

There are clear trends in the metal ratios in VMSDs with geologic age, such as lower Pb/Zn, Ba/Zn and Pb/(Pb + Zn + Cu) ratios in the older VMSDs (Fig. 25). Note that the data in Fig. 23 are only for deposits associated with *felsic* volcanic rocks; those associated with mafic to intermediate volcanic rocks are excluded. A trend of decreasing Pb/Ag ratios with increasing age of VMSDs has also been suggested (Franklin et al., 1981). Such trends have been explained traditionally by a model postulating a continuous increase in the Pb content of magmas (and the entire upper crust) through geologic time (e.g., Hutchinson, 1973). However, the analyses of Archean felsic volcanic rocks in the Abitibi belt by Goodwin (1977) and by us (unpublished data) indicate that their trace metal contents, including Cu, Zn, Pb and Ag, are essentially the same as those in the Miocene volcanic rocks in the Hokuroku district.

An alternative explanation to igneous rock type for the secular trend in the metal ratios of VMSDs is to attribute them to generally higher thermal gradients in the Archean hydrothermal systems (Ohmoto, 1985). As discussed in the section on "Chemical evolution of a growing massive ore body", during the maturation of massive sulfide ore from the primitive black ore to yellow ore, Pb and Ba is removed preferentially relative to Zn and Ag, causing the

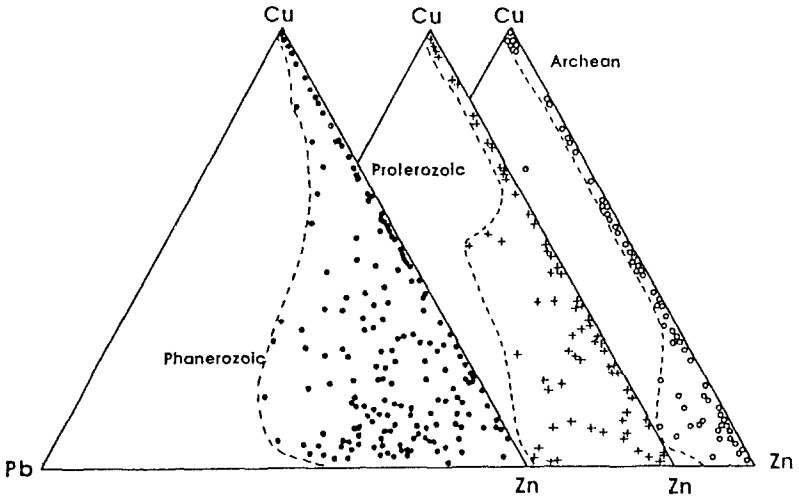

Fig. 25. Metal ratios of volcanogenic massive sulfide deposits associated with volcanic rocks of mostly felsic compositions. Data are from Anderson and Guilbert (1979), Divi et al. (1980), Franklin and Thorpe (1982), Donnelly and Hahn (1981), and Mosier et al. (1983).

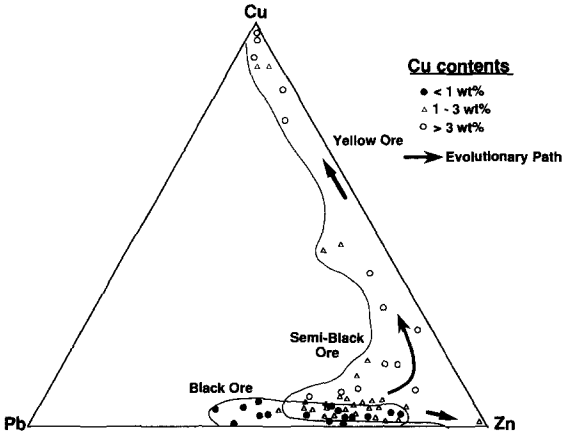

Fig. 26. Trends in metal ratios of Kuroko ores. Data are from Ishihara (1974) and Pavelka (1984). The arrows indicate trends during maturation of massive ores.

more mature ores to approach the Cu corner in the Cu–Pb–Zn ternary diagram along curved paths (Fig. 26). If the conversion of black ore to yellow ore was a simple addition of Cu, or if both sphalerite and galena were dissolved at the same rates, the metal ratios of yellow ores would plot on straight lines connecting the Cu corner and the black ore points in

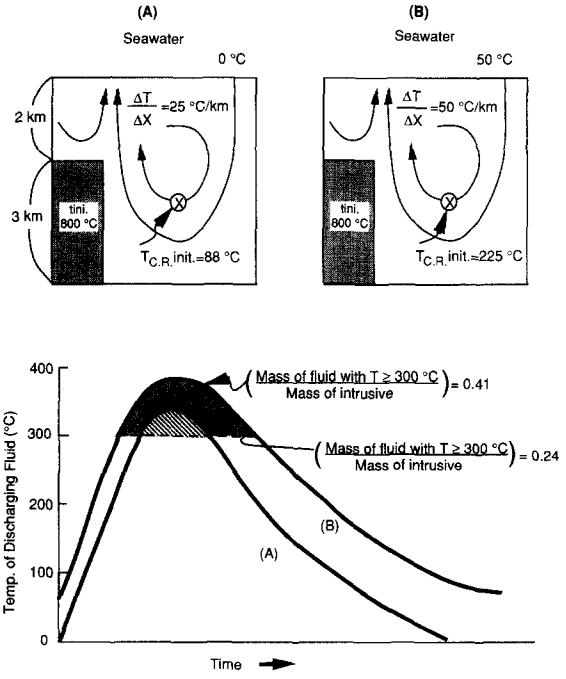

Fig. 27. Comparison of temperature–time curves for two submarine hydrothermal systems. (A): a typical setting for Kuroko systems, (B): a possible setting for Archean systems. Note that the amount of high temperature ($T > 300$°C) fluids discharged in (A) is about twice as much as that in (B).

Fig. 26. Thus, the observed secular trends in the metal ratios of VMSDs may reflect the development of more-mature type VMSDs in the Archean.

A possible cause of more-mature type VMSDs in the Archean earth is a higher thermal gradient in the seawater–rock systems. For example, an intrusive with an initial temperature of 800°C could circulate nearly twice as much fluid at $T \geq 300$°C if the initial seawater temperature were 50°C instead of the 0°C of present-day ocean-bottom water, and if the geothermal gradient were 50°C/km instead of 25°C/km (Fig. 27). The common occurrence of Fe-rich chlorite in the central alteration zone of Archean VMSDs associated with felsic volcanics, such as in the Abitibi belt, is also compatible with the above model because higher temperature fluids tend to contain higher Fe. Mg-rich chlorite that formed earlier in the central alteration zone at temperatures ~ 300°C could have been transformed to Fe-rich chlorite during the thermal maximum stage.

The proposition of warmer Archean oceans and higher geothermal gradients in the Archean crust has been made by various investigators. For example, the abundance of komatiite in the Archean has been attributed to higher geothermal gradients, which may be a result of higher heat flow and thinner crusts (e.g., Meyer, 1981; Annenhauser, 1981). The ocean-bottom temperatures of ~ 30°C for Archean oceans has been suggested by Ohmoto and Felder (1987) based on sulfur isotopic characteristics of biogenic pyrites in Archean sedimentary rocks. An oxygen isotope study of Archean cherts and phosphates by Karhu and Epstein (1986) suggests temperatures of > 80°C if isotopic equilibrium were established. Such temperatures may represent higher diagenetic temperatures in the sediments due to the combination of a warmer ocean and higher geothermal gradients.

Archean VMSDs are generally more matured than the Phanerozoic ones. However, there are some Archean VMSDs, such as the ~ 3.5 b.y. old Big Stubby deposit in the Pilbara district, Australia that have the mineralogical and elemental characteristics of the least matured Kuroko ores (i.e., chert + hematite + barite + galena + sphalerite + pyrite) (Samieyani and Ohmoto, 1996). These deposits are much smaller than the Cu-rich VMSDs of the Archean ages. The occurrences of such smaller and Pb-rich VMSDs suggest that the formational processes of VMSDs have been basically the same since at least ~ 3.5 b.y. ago.

7. Conclusions and summary

The processes of formation of VMSDs have remained basically the same throughout geologic time. They were formed by hydrothermal fluids which were mostly contemporaneous seawater that had undergone extensive changes in temperature and composition through interaction with high-temperature country rocks. Igneous intrusions (~ 10 km^3 in size) beneath the seafloor caused heating of seawater (pore fluids) and the country rocks, and generated convective circulation of the pore fluids. The pore fluids acquired heavy metals by leaching of the country rocks. H_2S was produced by two processes: (1) initial fixation of seawater sulfate as disseminated gypsum or anhydrite in the country rocks, which was followed by dissolution, and reduction by Fe^{2+} and organic C from the country rocks; and (2) leaching of sulfide from the country rocks.

VMSDs grew on and/or very near the seafloor by two concurrent processes: (1) mixing of hot ore-forming fluids and cold seawater, which resulted in precipitation of the black-ore mineral assemblage; and (2) metasomatic reactions between the early-formed ore minerals with later, hotter fluids, which resulted in successive transformation of black ore to Cu-rich yellow ore, and then to massive pyrite ore. An important aspect was that the growth of ore bodies took place during the waxing stage of hydrothermal activity.

The differences in size, geometry, mineralogy, metal ratios, and the isotopic compositions of VMSDs were caused by the differences in the *environmental parameters* of the ore-forming systems, especially the temperature and composition (Cl^-, O_2 and SO_4^{2-} contents) of seawater; the mineralogy, chemistry and thermal structure of the country rocks; and the size and type of intrusives that acted as the heat source. All these environmental parameters depend on the tectonic and paleogeographic setting. All VMSDs appear to have formed in extensional tectonic regimes.

For hydrological, physical and geochemical reasons, submarine depressions, especially those created

by submarine caldera formation and/or by large-scale tectonic processes (e.g., rifting) in the equatorial regions, become most favorable sites for the formation of large VMSDs and other submarine hydrothermal deposits (shale/carbonate hosted massive sulfide deposits and banded iron formations). Therefore, an identification, through isopach map analyses of tuffs, tuff breccia, mudstones, and evaporites in submarine volcanic terrains, of large submarine depressions may be an effective approach in the exploration of new VMSDs.

Acknowledgements

An earlier version of this manuscript was prepared as a review paper on "Volcanogenic Massive Sulfide Deposits (VMSDs)" for inclusion in an ill-fated publication from the NATO Advanced Institute on Hydrothe⌘"rmal Ore Deposits, held in Salamanca, Spain in 1987. Since then, the manuscript has been modified several times and used as a lecture note for short courses given at various academic and industrial institutions. An invitation to present a synthesis of "Submarine hydrothermal mineralization" at the Solomon Symposium held in Perth, Australia, in September, 1994, has given me a final incentive needed to complete this manuscript for publication. Critical reviews of the earlier manuscript by Al Guber, Hu Barnes, Mike Solomon, and John Walshe have contributed significantly to improve the manuscript. Especially, the comments from Mike Solomon are greatly appreciated. Assistance by Y. Watanabe in the preparation of this manuscript is gratefully acknowledged. This paper represents parts of research supported by the National Science Foundation under grant numbers EAR-8319402, EAR-8508379, EAR-9004813, and EAR-9003554, and grants from the Japanese Ministry of Science, Culture and Education.

References

Amann, H. Bäcker, H. and Blissenbach, E., 1973. Metalliferous muds of the marine environment. Offshore Technology Conf., Houston, Tex., Preprint (OTCPA4), 1(5): 345–353.

Annenhauser, C.R., 1981. The relationship of mineral deposits to early crustal evolution. Econ. Geol., 75th Anniv. Vol.: 42–64.

Anderson, P. and Guilbert, J.M., 1979. The Precambrian massive sulfides of Arizona — A district metallogenic epoch and province. In: Papers on Mineral Deposits of Western North America. Nev. Bur. Mines Geol., Rept. 33: 39–48.

Baker, E.T. and Lupton, J.E., 1990. Changes in submarine ^{3}He/heat ratios as an indicator of magmatic/tectonic activity. Nature, 346: 556–558.

Barton, P.B., Jr., 1978. Some ore textures involving sphalerite from the Furutobe mine, Akita Prefecture, Japan. Min. Geol., 28: 293–300.

Barton, P.B., Jr. and Bethke, P.M., 1987. Chalcopyrite decease in sphalerite: Pathology and epidemiology. Am. Mineral., 72: 451–467.

Beaty, D.W. and Taylor, H.P., Jr., 1982. Some petrologic and oxygen isotopic relationships in the Amulet mine, Noranda, Quebec, and their bearing on the origin of Archean massive sulfide deposits. Econ. Geol., 77: 95–108.

Bluth, G. and Ohmoto, H., 1986. Sulfur isotope geochemistry of hydrothermal vent sites from the East Pacific Rise at 13°N. Abstr. Progr., Geol. Soc. Am., Ann. Meet., San Antonio, Tex., 611 pp.

Burnham, C.W. and Ohmoto, H., 1980. Late-stage processes of felsic magmatism. Soc. Min. Geol. Jpn., Spec. Iss., 8: 1–11.Burnham

Cammeron, E.M. and Hattori, K., 1985. The Hemlo gold deposit, Ontario: A geochemical and isotopic study. Geochim. Cosmochim. Acta, 49: 2041–2050.

Campbell, I.H., McDougall, T.J. and Turner, J.S., 1984. A note on fluid dynamic processes which can influence the deposition of massive sulfides. Econ.Geol., 79: 1905–1913.

Casadevall, T. and Ohmoto, H., 1977. Sunnyside mine, Eureka mining district, San Juan County, Colorado: Geochemistry of gold and base metal ore deposition in a volcanic environment. Econ. Geol., 72: 1285–1320.

Cathles, L.M., 1983. An analysis of the hydrothermal system responsible for massive sulfide deposits in the Hokuroku Basin of Japan. Econ. Geol., Monogr. 5: 439–487.

Cathles, L.M., 1993. A capless 350°C flow zone model to explain megaplumes, salinity variations, and high-temperature veins in ridge axis hydrothermal systems. Econ. Geol., 88: 1977–1988.

Costa, U.R., Barnett, R.L. and Kerrich, R., 1983. The Mattagami Lake mine Archean Zn–Cu sulfide deposit, Quebec: Hydrothermal coprecipitation of talc nd sulfides in a sea-floor brin pool — evidence from geochemistry, $^{18}O/^{16}O$, and mineral chemistry. Econ. Geol., 78: 1144–1203.

Craig, H., Welham, J.A., Kim, K., Poreda, R. and Lupton, J.E., 1980. Geochemical studies of 21°N EPR hydrothermal fluids. EOS, Trans. Am. Geophys. Union, 61: 992.

Date, J., Watanabe, Y. and Saeki, Y., 1983. Zonal alteration around the Fukazawa Kuroko deposits, Akita Prefecture, Jpn. Econ. Geol., Mon. 5: 365–386.

Degens, E.T. and Ross, D.A. (Editors), 1969. Hot brines and recent heavy metal deposits in the Red Sea. Springer Verlag, New York, N.Y., 600 pp.

Divi, S.R., Thorpe, R.I. and Franklin, J.M., 1980. Use of discriminant analysis to evaluate compositional control of stratiform massive sulfide deposits in Canada. Can. Geol. Surv., Pap. 79-20: 23 pp.

Donnelly, M.E. and Hahn, G.A., 1981. A review of the Precambrian volcanogenic massive sulfide deposits in central Arizona and the relationship to their depositional environment. In: Relations to Tectonics to Ore Deposits in the Southern Cordillera. Ariz. Geol. Surv. Digest, XIV: 11–21.

Drummond, S.E., 1981. Boiling and mixing of hydrothermal fluids: chemical effects on mineral precipitation. Ph.D. thesis, The Pennsylvania State Univ., University Park, Pa.

Edmond, J.M., Measures, C., Mangum, B., Sclater, F.R., Collier, R. and Hudson, A., 1979. On the formation of metal-rich deposits at ridge crests. Earth Planet. Sci. Lett., 46: 19–30.

Eldridge, C.S., Barton, P.B., Jr. and Ohmoto, H., 1983. Mineral textures and their bearing on formation of the Kuroko orebodies. Econ. Geol., Monogr. 5: 241–281.

Eldridge, C.S., 1984. A sulfur isotopic, ore textural, chemical, and experimental study on the formation of the Kuroko deposits, Hokuroku district, Japan. Ph.D. thesis, The Pennsylvania State Univ., University Park, Pa.

Evans, W.C., White, L.D. and Rapp, J.B., 1988. Geochemistry of some gases in hydrothermal fluids from the southern Juan de Fuca Ridges. J. Geophys. Res., 93: 15305–15313.

Fehn, U., Doe, B.R. and Delevaux, M.H., 1983. The distribution of lead isotopes and the origin of Kuroko ore deposits in the Hokuroku district, Jpn. Econ. Geol., Monogr. 5: 488–506.

Francheteau, J., Needham, H.D., Choukroune, P., Juteau, T., Seguret, M., Ballard, R.D., Fox, P.J., Normark, W., Carranza, A., Cordoba, D., Guerrero, J., Rangin, C., Bougault, H., Cambon, P. and Hékinian., 1979. Massive deep-sea sulphide ore deposits discovered on the East pacific Rise. Nature, 277: 523–528.

Franklin, J.M., Lydon, J.W. and Sangster, D.F., 1981. Volcanic-associated massive sulfide deposits. Econ. Geol., 75th Anniv. Vol.: 485–627.

Franklin, J.M. and Thorpe, R.I., 1982. Comparative metallogeny of the Superior, Slave and Churchill Provinces. In: R.W. Hutchinson, C.D. Spence and J.M. Franklin (Editors), Geol. Assoc. Can., Spec. Pap., 25: 3–90.

Geer, K.A., 1988. Geochemistry of the stratiform zinc–lead–barite mineralization at the Meggen mine, Federal Republic of Germany. Ph.D. thesis, The Pennsylvania State Univ., University rk, Pa.

Goodfellow, W.D. and Franklin, J.M., 1993. Geology, mineralogy, and chemistry of sediment-hosted clastic massive sulfides in shallow cores, middle valley, northern Juan de Fuca Ridge. Econ. Geol., 88: 2037–2068.

Goodwin, A.M., 1977. Archean volcanism in Superior Province, Canadian Shield. Geol. Assoc. Canada, Spec. Pap., 16: 205–241.

Goldfarb, M.S., Converse, D.R., Holland, H.D. and Edmond, J.M., 1983. The genesis of hot spring deposits on the East Pacific Rise, 21°N. Econ. Geol., Monogr. 5: 184–198.

Graham, U.M., Bluth, G. and Ohmoto, H., 1988. Sulfide–sulfate chimneys on the East Pacific Rise, 11° and 13°N latitudes. Part I: mineralogy and paragenesis. Can. Mineral., 26: 487–504.

Graham, U.M. and Ohmoto, H., 1994. Experimental study of fomation mechanisms of hydrothermal pyrite. Geochim. Cosmochim. Acta, 58: 2187–2202.

Green, G.R., Ohmoto, H., Date, J. and Takahashi, T., 1983. Whole-rock oxygen isotope distribution in the Fukazawa–Kosak area, Hokuroku district, Japan, and its potential application to mineral exploration. Econ. Geol., Monogr. 5: 395–411.

Guber, A.L. and Green, G.R., 1983. Aspects of the sedimentologic and structural development of the eastern Hokuroku district, Japan. Econ. Geol., Monogr. 5: 71–95.

Guber, A.L. and Merrill, S.M., III, 1983. Paleobathymetric significance of the foraminifera from the Hokuroku district. Econ. Geol., Monogr. 5: 55–70.

Guilbert, J.M. and Park, C.F., Jr., 1986. The Geology of Ore Deposits. Freeman, New York, N.Y., 985 pp.

Gustafson, L.B. and Williams, N., 1981. Sediment-hosted stratiform deposits of copper, lead, and zinc. Econ. Geol., 75th Anniv. Vol.: 139–178.

Harley, D.N., 1979. A mineralized Ordovician resugent caldera complex in the Bathurst–Newcastle mining district, New Brunswick, Canada. Econ. Geol., 74: 786–796.

Hashiguchi, H., 1983. Penecontemporaneous deformation of Kuroko ore at the Kosaka mine, Akita, Japan. Econ. Geol., Monogr. 5: 167–183.

Hashiguchi, H., Yamada, R. and Inoue, T., 1983. Practical application of low Na_2O anomalies in footwall acis lava for delimiting promising areas around the Kosaka and Fukazawa Kuroko deposits, Akita Prefecture, Japan. Econ. Geol., Monogr. 5: 387–394.

Hattori, K. and Sakai, H., 1979. D/H ratios, origins and evolution of the ore-forming fluids for the Neogene veins and Kuroko deposits of Japan. Econ. Geol., 74: 535–555.

Hattori, K. and Muehlenbachs, K., 1980. Marine hydrothermal alteration at a Kuroko ore deposit, Kosaka, Japan. Contrib. Mineral. Petrol., 74: 285–292.

Hayashi, K. and Ohmoto, H., 1991. Solubility of gold in NaCl- and H_2S-bearing aqueous solutions at 250–350°C. Geochim. Cosmochim. Acta, 55: 2111–2126.

Haymon, R.M. and Kastner, M., 1981. Hot spring deposits on the East Pacific Rise at 21°N: Preliminary description of mineralogy and genesis. Earth Planet. Sci. Lett., 53: 363–381.

Heaton, T.H.E. and Spooner, S.M.F., 1977. Hydrogen and oxygen isotope evidence for seawater–hydrothermal alteration and ore deposition, Troodos, Cyprus. In: Volcanic Processes in Ore Genesis. Inst. Mining Metall. London, pp. 42–57.

Holland, H.D., 1978. The Chemistry of the Atmosphere and Oceans. Wiley, New York, NY, 351 pp.

Holland, H.D. and Malinin, S.D., 1979. The solubility and occurrence of non-ore minerals. In: H.L. Barnes (Editor), Geochemistry of Hydrothermal Ore Deposits, 2nd ed. Wiley, New York, N.Y., pp. 461–508.

Horikoshi, E., 1969. Volcanic activity related to the formation of the Kuroko-type deposits in the Kosaka district, Japan. Mineral. Deposita, 4: 321–345.

Hoy, L., 1993. Regional evolution of hydrothermal fluids in the Noranda district, Qubec: evidence from $\delta^{18}O$ values from volcanogenic massive sulfide deposits. Econ. Geol., 88: 1526–1541.

Hutchinson, R.W., 1973. Volcanogenic sulfide deposits and their metallogenic significance. Econ. Geol., 68: 1223–1246.

Ijima, A., 1974. Clay and zeolite zones surrounding Kuroko deposits in the Hokuroku district, northeast Japan. Soc. Min. Geol. Jpn., Spec. Issue 6: 267–290.

Ishihara, S. (Editor), 1974. Geology of the Kuroko Deposits. Soc. Min. Geol. Jpn., Spec. Issue 6, 437 pp.

Karhu, J. and Epstein, S., 1986. The implication of the oxygen isotope records in coexisting cherts and phosphates. Geochim. Cosmochim. Acta, 50: 1745–1756.

Kennedy, B.M., 1988. Noble gasess in vent water from the Juan de Fuca Ridge. Geochim. Cosmochim. Acta, 52: 1929–1935.

Kumita, K., Hashimoto, E., Yamada, M. and Sasaki, M., 1983. The formational environment of the Shakanai ore deposit. Min. Geol., 32: 225–242 (in Japanese).

Lambe, R.N. and Rowe, R.G., 1987. Volcanic history, mineralization, and alteration of the Crandon massive sulfide deposit, Wisconsin. Econ. Geol., 82: 1204–1238.

Lawrence, J.R. and Gieske, J.M., 1981. Constraints on water transport and alteration in the oceanic crust from the isotopic composition of pre water. J. Geophys. Res., 86: 7924–7934.

Lenagh, T., 1985. Areal distribution and strontium contents of anhydrites peripheral to Kuroko massive sulfide deposits in Japan and their implications for hydrothermal fluid circulation. M. Sc. thesis, The Pennsylvania State Univ., University Park, Pa.

Li, B. and Manuel, O.K., 1994. A noble gas technique for the identification of mantle and crustal materials and its application to the Kuroko deposits. Geochem. J., 28: 47–69.

Lloyd, E.F., Glasby, G.P. and Glover, R.B., 1976. Atlantis II and Danakil Depression brines: a comparison. Geol. Jahrb., D17: 187–196.

Melivat, L., Pineau, F. and Javoy, M., 1987. Hydrothermal vent waters at 13°N on the East Pacific Rise: isotopic composition and gas concentration. Earth Planet. Sci. Lett., 84: 100–108.

Meyer, C., 1981. Ore forming processes in geologic history. Econ. Geol., 75th Anniv. Vol.: 6–41.

Miller, A.R., Desmore, C.D., Degens, E.T., Hathaway, J.C., Manheim, F.T., McFarlin, P.F., Pocklington, H. and Jokela, A., 1966. Hot brines and recent iron deposits in deeps of the Red Sea. Geochim. Cosmochim. Acta, 30: 341–359.

Mizukami, M. and Ohmoto, H., 1983. Controlling mechanisms for the major element chemistry of aqueous solutions in tuff-rich environments. Econ. Geol., Monogr. 5: 559–569.

Morton, R.L., Walker, J.S., Hudak, G.J. and Franklin, J.M., 1991. The early development of an Archean submarine caldera complex with emphasis on the Mattabi ash-flow tuff and its relationship to the Mattabi massive sulfide deposit. Econ. Geol., 86: 1002–1011.

Mosier, D.L., Singer, D.A. and Salem, B.B., 1983. Geologic and grade-tonnage information on volcanic-hosted copper–zinc–lead massive sulfide deposits. USGS Open File Rep., 83-89, 77 pp.

Mottl, M.J. and Holland, H.D., 1978. Chemical exchange during hydrothermal alteeration of basalty seawater. I. Experimental results for major and minor components of seawater. Geochim. Cosmochim. Acta, 42: 1103–1117.

Muehlenbachs, K., 1980. The alteration and aging of the basaltic layer of the seafloor: Oxygen isotopic evidence from DSDP/IPOD legs 51, 52, and 53. Deep Sea Drilling Project, Initial Rep., Vol. 51, 52, 53, Part 2: 1159–1167.

Munha, J., Barriga, F.J.A.S. and Kerrich, R., 1986. High ^{18}O ore-forming fluids in volcanic-hosted base metal massive sulfide deposits: geologic, $^{18}O/^{16}O$, and D/H evidence from the Iberian pyrite belt; Crandon, Wisconsin; and Blue Hill, Maine. Econ. Geol., 81: 53–552.

Murowchick, J.B. and Barnes, H.L., 1986. Marcasite precipitation from hydrothermal solutions. Geochim. Cosmochim. Acta, 50: 2615–2629.

Ohashi, R., 1919. On the origin of the Kuroko of the Kosaka mine. Geol. Soc. Tokyo J., 26: 107–132 (in Japanese).

Ohmoto, H., 1978. Submarine calderas: A key to the formation of volcanogenic massive sulfide deposits? Min. Geol., 28: 215–217.

Ohmoto, H., 1983. Geologic setting of the Kuroko deposits, Japan: Part I. geologic history of the Green Tuff Region. Econ. Geol., Monogr. 5: 9–23.

Ohmoto, H., 1985. Thermodynamic and kinetic evaluation of the causes of metal-ratio regularities in low temperature hydrothermal deposits. Geol. Soc. Am., Abstr. Progr., 17, 614 pp.

Ohmoto, H., 1986a. Stable isotope geochemistry of ore deposits. In: J.W. Valley, H.P. Taylor, Jr. and J.R. O'Neil (Editors), Stable Isotopes in High Temperature Geological Processes. Reviews in Mineralogy Vol. 16, Mineral. Soc. Am., pp. 491–560.

Ohmoto, H., 1986b. Systematics of metal ratios and sulfur isotopic ratios in low-temperature basemetal deposits. Terra Cognita, 6: 134–135.

Ohmoto, H., 1992. Biogeochemistry of sulfur and the mechanisms of sulfide–sulfate mineralization in Archean oceans. In: Schidlowski et al. (Editors), Early Organic Evolution: Implications for Mineral and Energy Resources. Springer, Berlin, pp. 378–397.

Ohmoto, H. and Felder, R.P., 1987. Bacterial activity in warmer, sulphate-bearing, Archaean oceans. Nature, 328: 244–246.

Ohmoto, H. and Goldhaber, M., 1996 Applications of sulfur and carbon isotopes in ore deposit research. In: H.L. Barnes (Editor), Geochemistry of Hydrothermal Ore Deposits, 3rd ed. Wiley, New York, N.Y. (in review).

Ohmoto, H. and Lasaga, A.C., 1982. Kinetics of reactions between aqueous sulfates and sulfides in hydrothermal systems: Geochim. Cosmochim. Acta, 46: 1727–1745.

Ohmoto, H. and Rye, R.O., 1974. Hydrogen and oxygen isotopic compositions of fluid inclusions in the Kuroko deposits, Japan. Econ. Geol., 69: 947–953.

Ohmoto, H. and Rye, R.O., 1979. Isotopes of sulfur and carbon. In: H.L. Barnes (Editor), Geochemistry of Hydrothermal Ore Deposits, 2nd ed. Wiley, New York, N.Y., pp. 509–567.

Ohmoto, H. and Skinner, B.J. (Editors), 1983. The Kuroko and related volcanogenic massive sulfide deposits. Econ. Geol., Monogr. 5, 604 pp.

Ohmoto, H. and Takahashi, T., 1983. Geologic setting of the Kuroko Deposits, Japan. Part III. Submarine calderas and Kuroko genesis. Econ. Geol., Monogr. 5: 39–54.

Ohmoto, H., Kajiwara, Y. and Date, J., 1970. The Kuroko ores in

Japan: products of seawater? Annu. Meet., Geol. Soc. Am., Milwaukee, Wisc., Abstr. Progr., 640 pp.

Ohmoto, H., Mizukami, M., Drummond, S.E., Eldridge, C.S., Pisutha-Arnond, V. and Lenagh, T.C., 1983. Chemical processes of Kuroko formation. Econ. Geol., Monogr. 5: 570–604.

Ohmoto, H., Kaiser, C.J. and Geer, K.A., 1991. Systematics of sulphur isotopes in recent marine sediments and ancient sediment-hosted basemetal deposits. In: H.M. Herbert (Editor), Stable Isotopes and Fluid Processes in Mineralisation. Geol. Soc. Aust., Spec. Publ., 13.

Ohmoto, H., Kakegawa, T. and Lowe, D.R., 1993. 3.4-billion-year-old biogenic pyrites from Barberton, South Africa: Sulfur isotope evidence. Science, 262: 555–557.

Pavelka, A., 1984. Trends in metal ratios as a function of ore type and stratigraphic position in the Kuroko deposits, Japan. M. Sc. thesis, The Pennsylvania State University, University Park, Pa., 160 pp.

Pisutha-Arnond, V. and Ohmoto, H., 1983. Thermal history, and chemical and isotopic compositions of the ore-forming fluids responsible for the Kuroko massive sulfide deposits in the Hokuroku district of Japan. Econ. Geol., Monogr. 5: 523–558.

Pottorf, R.J. and Barnes, H.L., 1983. Mineralogy, geochemistry, and ore genesis of hydrothermal sediments fom the Atlantis II Deep, Red Sea. Econ. Geol., Monogr. 5: 198–223.

Rimstidt, J.D. and Barnes, H.L., 1980. The kinetics of silica–water reactions. Geochim. Comochim. Acta, 44: 1683–1699.

Ripley, E.M. and Ohmoto, H., 1977. Mineralogic, sulfur isotope, and fluid inclusion studies of the stratabound copper deposits of the Raul mine, Peru. Econ. Geol., 72: 1017–1041.

Rona, P.A., 1988. Hydrothermal mineralization at ocean ridges. Can. Mineral., 26: 431–466.

Rona, P.A. and Scott, S.D., 1993. A special issue on sea-floor hydrothermal mineralization: new perspectives. Preface. Econ. Geol., 88: 1933–1976.

Rose, A.W., Barnes, H.L., Burnhamn C.W. and Ohmoto, H., 1977. Report on workshop on Research Frontiers in Exploration for Non-Renewable Resources. A report to the Division of Advanced Energy and Resources Research and Technology. Natl. Sci. Found., Washongton, D.C., 164 pp.

Samieyani, A. and Ohmoto, H., 1996. The 3.5 Ga Kuroko-type volcanogenic massive sulfide deposit at the Big Stubby Prospect, Western Australia (in prep.).

Sangster, D.F., 1968. Relative sulfur isotope abundances of ancient seas and strata-bound sulfide deposits. Geol. Assoc. Can., Proc., 19: 79-86.

Sangster, D.F. and Scott, S.D., 1976. Precambrian strata-bound, massive Cu–Zn–Pb sulfide ores of North America. In: K.H. Wolf (Editor), Cu, Zn, Pb, and Ag Deposits. Handbook of Strata-Bound and Stratiform Ore Deposits, Vol. 6. Elsevier, Amsterdam, pp. 129–222.

Sato, T., 1972. Behaviors of ore-forming solutions in seawater. Min. Geol., 22: 31–42.

Sato, T., 1973. A chloride complex model for Kuroko mineralization. Geochem. J., 7: 245–270.

Schoonen, M.A. and Barnes, H.L., 1991. Reactions forming pyrite and marcasite from solutions: II Via FeS precursors below 100°C. Geochim. Cosmochim. Acta, 55: 1505–1514.

Scott, S.D., 1978. Structural control of the Kuroko deposits of the Hokuroku district, Japan. Min. Geol., 28: 301–312.

Seccombe, P.K., 1977. Sulphur isotope and trace metal composition of stratiform sulphides as an ore guide in the Canadian Shiled. J. Geophys. Explor., 8: 117–137.

Shanks, W.C., III. and Bischoff, J.L., 1980. Geochemistry, sulfur isotope composition, and accumulation rates of the Red Sea geothermal deposits. Econ. Geol., 75: 445–459.

Smith, P.E., Schandl, E.S. and York, D., 1993. Timing of metasomatic alteration of the Archean Kidd Creek massive sulfide deposite, Ontario, using $^{40}Ar-^{39}$ Ar laser dating of single crystals of fuchsite. Econ. Geol., 88: 1636–1642.

Solomon, M., 1976, "Volcanic" massive sulphide deposits and their host rocks — a review and an explanation. In K.H. Wolf (Editor), Regional Studies and Specific Deposits. Handbook of Strata-bound and Stratiform Ore Deposits, Vol. 2. Elsevier, Amsterdam, pp. 21–50.

Solomon, M. and Walshe, J.L., 1979. The formation of massive sulfide deposits on the seafloor. Econ. Geol., 74: 797–813.

Solomon, M., Walshe, J.L. and Eastoe, C.J., 1987. Experiments on convection and their relevance to the genesis of massive sulfide deposits. Aust. J. Earth Sci., 34: 311–323.

Spooner, E.T.C. and Fyfe, W.S., 1973. Sub-sea floor metamorphism, heat and mas transfer. Contrib. Mineral. Petrol., 42: 287–304.

Styrt, M.M., Brackmann, A.J., Holland, H.D., Clark, B.C., Pisutha-Arnond, V., Eldridge, C.S. and Ohmoto, H., 1981. The mineralogy and isotopic composition of sulfur in hydrothermal sulfide/sulfate deposuts on the East Pacific Rise, 21°N latitude. Earth Planet. Sci. Lett., 53: 282–290.p

Tanimura, S., Date, J., Takahashi, T. and Ohmoto, H., 1983. Geologic setting of the Kuroko deposits, Japan. Part II. Stratigraphy and structure of the Hokuroku district. Econ. Geol., Monogr. 5: 24–38.

Tsutsumi, T. and Ohmoto, H., 1983. A preliminary oxygen isotope study of tetsusekiei ores associated with Kuroko deposits in the Hokuorku district, Japan. Econ. Geol., Monogr. 5: 433–438.

Urabe, T., 1987. Kuroko deposit modeling based on magmatic hydrothermal theory. Min. Geol., 37: 159–176.

Urabe, T., Scott, S.D. and Hattori, K., 1983. A comparison of footwall–rock alteration and geothermal systems beneath some Japanese and Canadian volcanogenic massive sulfide deposits. Econ. Geol., Monogr. 5: 345–364.

Utada, M., Tokoyo, T. and Aoki, H., 1981. The distribution of alteration zones in the central area of the Hokuroku district, northeastern Japan. Min. Geol., 31: 13–25.

Von Damm, K.L., 1990. Seafloor hydrothermal activity: black smoker chemistry and chimneys. Annu. Rev. Earth Planet. Sci., 18: 173–204.

Walker, R.R., Matulich, A., Amos, A.C., Watkins, J.J. and Mannard, G.W., 1975. The geology of the Kidd Creek mine. Econ. Geol., 70: 80–89.

Wedepohl, K.H. (Editor), 1969. Hand Book of Geochemistry Vol. I, II/2 and II/5. Springer, Berlin.

Zierenberg, R.A. and Shanks, W.C., III., 1988. Isotopic studies of epigenetic features in metalliferous sediment, Atlantis II Deep, Red Sea. Econ. Geol., 26: 737–753.